CEPSTRAL DOMAIN DECONVOLUTION OF MARINE SEISMIC REAL DATA

A DISSERTATION
submitted in partial fulfilment of
the requirements for the award of the Degree
of
MASTER OF TECHNOLOGY
in
APPLIED GEOPHYSICS

by
A. SANKARANKUTTY NAIR

DEPARTMENT OF GEOLOGY AND GEOPHYSICS
UNIVERSITY OF ROORKEE
ROORKEE (INDIA)
October, 1977

CERTIFICATE

CERTIFIED that the dissertation entitled, " CEPSTRAL DOMAIN DECONVOLUTION OF MARINE SEISMIC REAL DATA ", which is being submitted by Mr. A. SATHARANKUTTY NAIR in partial fulfilment for the award of the degree of M.Tech. in APPLIED GEOPHYSICS of the University of Roorkee, Roorkee is a record of student's own work carried out by him under our supervision and guidance. The matter embodied in the dissertation has not been submitted for the award of any other degree or diploma.

It is further certified that he has worked on this problem from January to September 1977.

V.K.GAUR,
PROFESSOR OF GEOPHYSICS,
DEPTT. OF GEOLOGY AND GEOPHYSICS,
UNIVERSITY OF ROORKEE,
ROORKEE, U.P.

P.S.MOHANIR,
READER,
DEPTT. OF GEOLOGY AND GEOPHYSICS,
UNIVERSITY OF ROORKEE,
ROORKEE, U.P.

Dated 14th October, 1977.

ACKNOWLEDGEMENT

It has been my proud privilege to work as a student with Dr. V.K.Gaur and Dr. P.S. Mohapir. Their untiring patience, constant guidance and kind help are largely responsible for the work presented in this dissertation.

Dr. L.Narasimha, Visiting Professor from University of Western Ontario, Canada; Dr. S.K.Upadhyay, Reader, Dept. of Geology and Geophysics and Dr. N.C.Joshi, Dr.S.Chakravarthy, Dept. of Electronics and Communications, University of Roorkee have provided very valuable suggestions and almsare help which I gratefully acknowledge.

I am deeply indebted to Dr.R.S.Mithal, Prof. and Head, Department of Geology and Geophysics, University of Roorkee, Roorkee, for providing necessary facilities to complete this work.

The work presented here could not have been possible without the co-operation of the staff at the Computer Center, Roorkee and Institute of Petroleum Exploration, Oil and Natural Gas Commission, Dehra Dun. It will be ungracious not to mention the names of Mr.V.C.Mohan, Mr.D.Das, Mr.M.C.Agarwal and Mr.S.Roy, who helped me in availing myself of the computer

facilities at IPE, Dehra Dun.

I am grateful to all my teachers in the department of Geology and Geophysics who taught me during the last 3 years.

Thanks are due to my friends Dr.K.C.Dolan, Dr.N.Ranganajan, Mr.N.Vijayakumar, Mr.P.K.Gupta, Mr.J.K.Pathak, Mr.D.P.Verma, Mr. Vyas and all others for their valuable assistance and co-operation at various occasions.

In the end I gratefully acknowledge the financial assistance received from the University Grants Commission in the form of Studentship during my M.Tech. Course.

16th October, 1977.

(A.SANKARANARAYANA MURTY NAIR)

PREFACE

For the past six to seven years Cepstral Domain Deconvolution has been given more attention as an alternative method for seismic deconvolution problems. This technique was primarily developed by Oppenheim, Schafer and Stockham[33]. Ulrych[33] applied this technique to seismology for the separation of convolved signals. The practical application of this technique in the field of seismic prospecting was discussed by Buhl, Stoffa, P. and Bryan[5,9,10]. In this dissertation this technique has been applied to recover the source wavelet and ground transmission response. The separation of the source wavelet and the ground transmission path response is carried out by windowing in the cepstral domain. We were able to separate source wavelet and the transmission path response and the results obtained are discussed in the fourth chapter.

CONTENTS

CHAPTER - I

INTRODUCTION

Deposits of petroleum and natural gas are located in reservoirs deep below the surface of the earth. In order to find these resources geophysical methods of exploration are used. The structures of the earth's crust, and the presence of ores, oil, coal and other minerals can be inferred from studies of the various physical phenomena taking place within the earth and on its surface.

Seismic prospecting is one of the most important methods of geophysical prospecting. The objective of seismic prospecting is to investigate the geological structure of the earth's crust based on the study of the propagation of elastic waves artificially created in it. The elastic waves caused by an explosion propagate in all directions penetrate into the crust to greater depths where they get reflected and refracted at the interfaces between the layers of rocks. After reflection or refraction within the earth the waves return to the surface where they are recorded by special instruments in the form of a seismogram. By determining the time of their transit and investigating the character of the ground vibrations, the depth and shape of the geological bounding plan at which reflection or refraction have occurred can be inferred. An idea can sometimes be found as to the composition of the rocks comprising these layers.

The difficulties which beset the seismic process are due to the interference and noise. Everything that is generated by the seismic source travelling over other than the desired paths (ie. the path followed by the primary reflections) can be termed interference and everything that is added to the seismic signal during the detecting, recording, and processing of the seismic data is noise. Noise is everything in the seismic data that is not related to the subsurface structure. The desired reflection signals, with noise superimposed, are detected and recorded. The problem is to identify the signal in the presence of the noise. Operations therefore must maximise the signal-to-noise ratio.

There are two principal ways to do this:

(a) To conduct the field operations so that a minimum of noise is generated, or the effects of noise are minimised during the recording process.

(b) To process the record data so as to reduce or eliminate the noise that is recorded.

The word 'signal' is a generic term that may denote the time variation of any physical quantity. For example, earth motion in seismic exploration may be referred to as a signal, the voltage records the earth motion is also a signal, and so is the actual recording on paper or on magnetic tape.

3

Before we can make any analysis or design equipment, we must first agree on how to characterize the signals. In this work we are interested in digital equipment. Therefore we shall assume that all the signals have been digitized, and then each signal is available in the form of a time series.

In seismic work there is always a distinction made between a wavelet and an arbitary seismic recording. Qualitatively a wavelet is a signal whose value is negligibly small except in some finite time interval. Thus a wavelet is special in the character. A wavelet can be represented by a sequence of amplitudes h_0, h_1, h_2, ... The subscripts denote the time with sampling interval normalized to unity. It is assumed that $h_i \doteq 0$, $i<0$ and that a wavelet has a finite energy.

Here we are interested to separate the source wavelet from the recorded seismogram.

Each seismic trace is a time series made up of reflected events together with various interfering waves and noise. The desired reflection events are the primary reflections, that is, waves that travel down to a given reflector and then back up to the surface where they are recorded.

An important type of undesirable interfering wave is the multiple reflection.

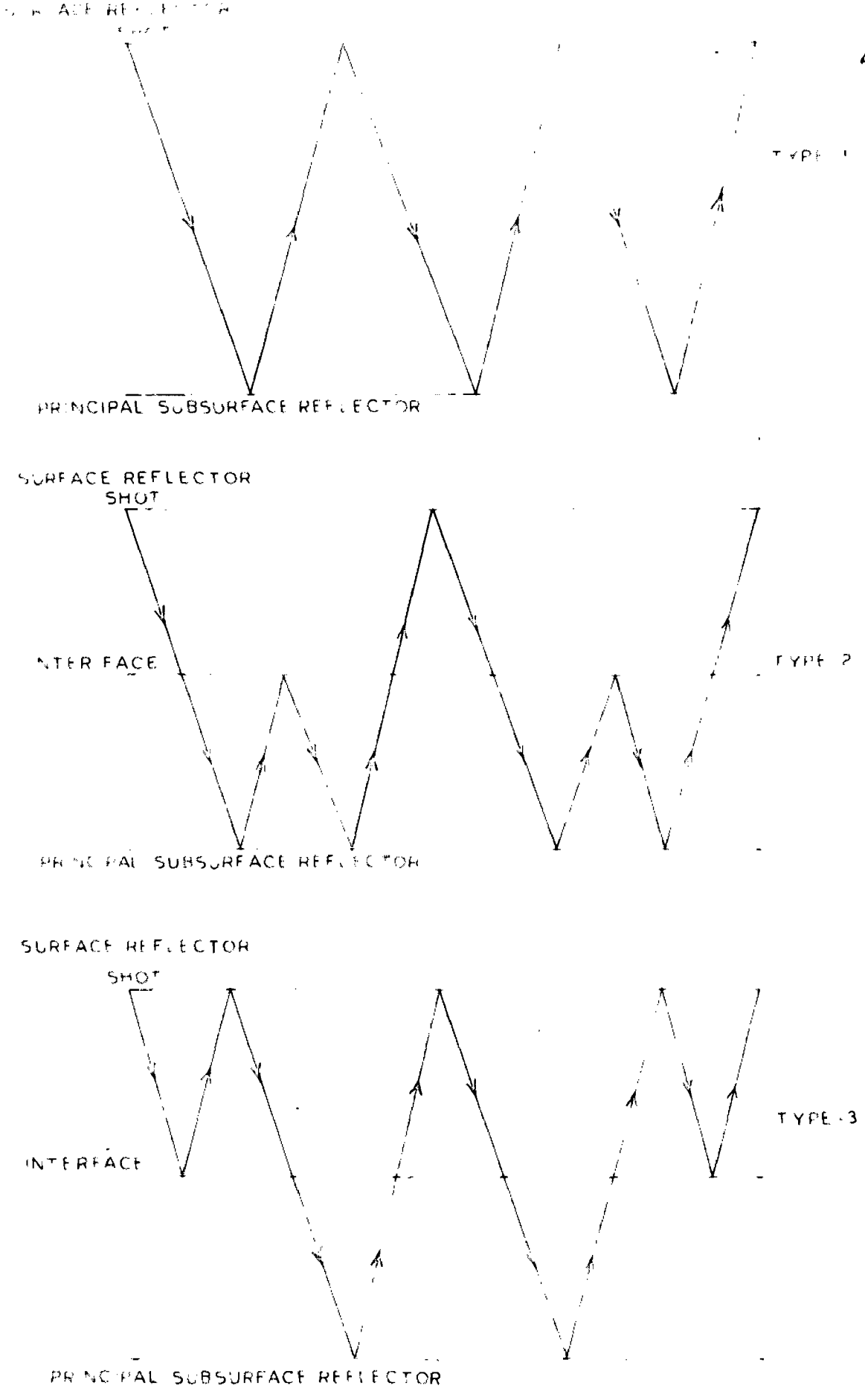

FIG 1 : MULTIPLE REFLECTION

A multiple reflection has a ray path that goes down to a given reflector, then up to another reflector and then down again to still another reflector and so on before it reaches to the surface as shown in the Fig.1.1.

In any layered system, there are many possible multiple reflections. The presence of multiple reflections make the identification of primary reflections difficult from the recorded seismic traces, and therefore it is necessary to process the traces so as to attenuate the multiples as much as possible.

A special kind of multiple reflection is the so-called reverberations or short-period multiple. Energy trapped in the near surface layers keeps getting reflected back and forth, and this energy becomes attached to the primary reflections as they travel through the near surface layers. As a result, instead of having sharp clear reflections with good time resolution, we have reflections followed by long reverberation trains. These trains overlap with the trains of succeeding primary reflections, and thus the whole seismic trace acquires a ringing or damped sinusoidal character. As a result it is difficult to pick out the onset of the primary reflections. The solution to this problem consists of annulling the energy in each reverberation trains but leaving intact the primary reflections, thus increasing the resolution of all the reflected events.

For the simplicity of explanation the signals are assumed to be continuous. However, all the processing is done for sampled signals and the required changes will be described at the appropriate places in the thesis.

Before we proceed, we need some concepts from linear system theory.

Let us first define some of the important terms:

1.1. Definitions:

1.1.1. Signals:- In the context of this work, the signal is any well behaved sequence of sample values.

1.1.2. System:- A system is a collection of physical devices that generates one or more signals, called the output signals, say $y_i(t)$, $i = 1,2, \ldots, M$; when stimulated by some other signals, called the input signals, say $x_j(t)$, $j = 1,2,3 \ldots N$. The input signals are also called the stimuli, and the output signals are also called the responses of the system.

Mathematically, the system can be represented by a set of relations

$$y_i(t) = F_i[x_1(t), x_2(t), \ldots, x_N(t)]$$

where $i = 1,2,\ldots, M$ (1.1)

For a single input single-output case, the equation (1.1) takes a simpler form

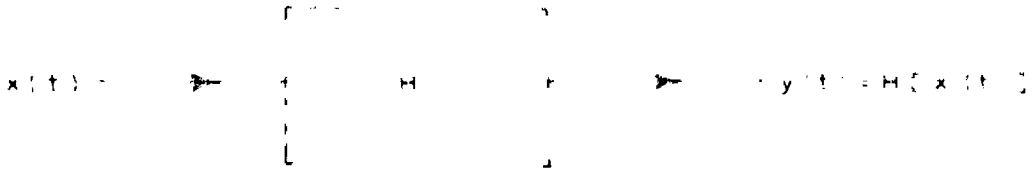

FIG. 1.2 SINGLE-INPUT SINGLE OUT-PUT SYSTEM

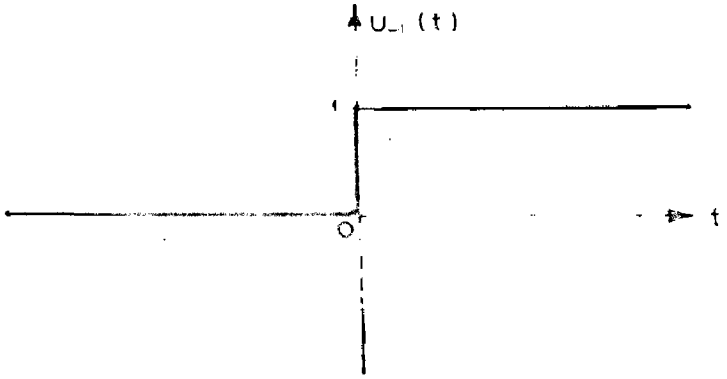

FIG 1.3 UNIT STEP

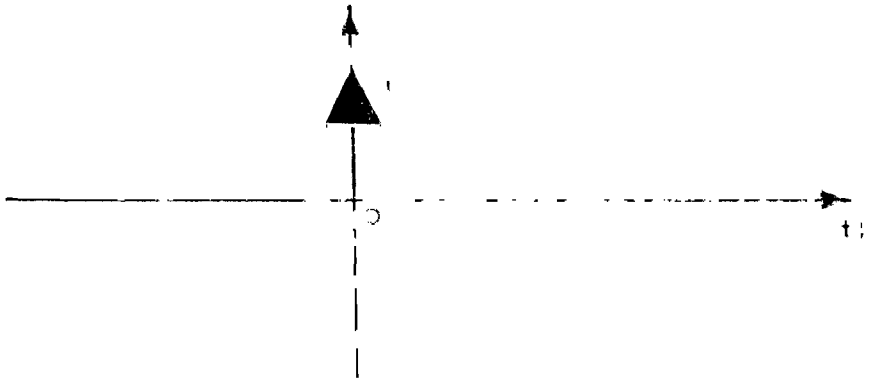

FIG 1.4 UNIT IMPULSE

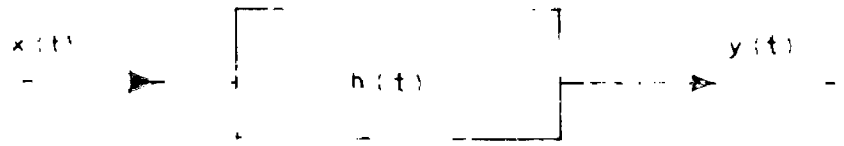

FIG 1.5 BLACK BOX REPRESENTATION OF CONVOLUTION

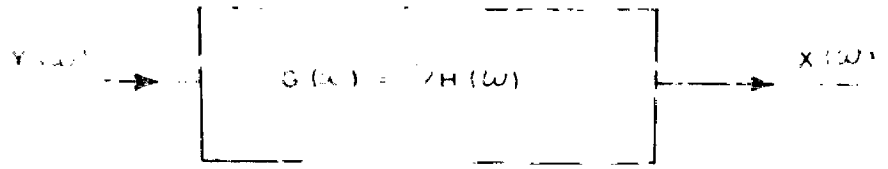

FIG 1.6 BLACK BOX REPRESENTATION OF DECONVOLUTION OR INVERSE FILTERING

$$y(t) = H[x(t)] \qquad (1.2)$$

as no suffices are needed.

The functional H is said to be a system operator and defines the system completely.

A single-input single-output system is shown in Fig.1.2.

1.1.3. Time-Invariant Systems- A system is said to be time-invariant if a time shifted input signal will yield a correspondingly time-shifted output signal. As an example, for a time-invariant system,

$$H[x(t)] = y(t) \text{ implies}$$
$$H[x(t+\tau)] = y(t+\tau) \qquad (1.3)$$

for all τ

A system is said to be time-varying otherwise.

1.1.4. Homogeneous System- A system is said to be homogeneous if the response of the system to a signal $ax(t)$ is equal to 'a' times the response of the system to the signal $x(t)$ for any constant 'a'. That is

$$H[ax(t)] = aH[x(t)] \qquad (1.4)$$

1.1.5. Additive Systems- A system is said to be additive if the response of the system to a signal $x_1(t) + x_2(t)$ is qual to the sum of the responses of the system to the signal $x_1(t)$ and $x_2(t)$.

$$H[x_1(t) + x_2(t)] = H[x_1(t)] + H[x_2(t)] \qquad (1.5)$$

1.1.6. Linear system:- A system is said to be linear if it is both homogeneous and additive. For example, if $x_1(t)$ and $x_2(t)$ are any input signals and a_1, a_2 are any constant then

$$H[a_1x_1(t) + a_2x_2(t)] = a_1H[x_1(t)] + a_2H[x_2(t)] \qquad (1.6)$$

1.1.7. Unit step:- Unit step denoted by $U_{-1}(t)$ is a continuous time function the value of which is 0 for $t<0$ and is 1 for $t>0$, as shown in Fig.1.3.

1.1.8. Unit Impulse:- We define the unit impulse to be the derivative of the unit step, denoted by $U_0(t)$. Graphically we use an arrow to denote the unit impulse, as shown in the Fig. 1.4.

1.1.9. Impulse Response:- The response of a linear, time-invariant system to the unit impulse $U_0(t)$ is known as the impulse response of the system and will be denoted as $h(t)$. That is if

$$x(t) = U_0(t) \qquad (1.7)$$

then $y(t) = H[U_0(t)] = h(t) \qquad (1.8)$

10

1.1.10. Fourier Transform:- It is possible to analyse the signal not directly but after suitable linear transformation. The transform-domain description of the signal has one to one correspondence to the time-domain description if the transform is invertible. One such linear transform which conducts the orthonormal decomposition of the signal in terms of the sinusoidal and cosinusoidal components. The fourier transform of the signal is referred to as the Fourier spectrum or simply spectrum of the signal. The Fourier transform relationships are

$$X(v) = \int_{-\infty}^{\infty} x(t)\, e^{-i2\pi ft}\, dt \qquad (1.9)$$

and

$$x(t) = \int_{-\infty}^{\infty} X(v)\, e^{i2\pi ft}\, df \qquad (1.10)$$

where $v = 2\pi f$. The independent variable f and v are referred to as the frequency and radian frequency respectively. Eq.(1.9) represents the transformation from the time domain to the frequency domain to and Eq.(1.10) represents the inverse transformation from the frequency domain to the time domain.

The definitions of Eqs.(1.9) and (1.10) assume that $\int_{-\infty}^{\infty} |x(t)|\, dt < \infty \qquad (1.11)$

i.e., that the signal is absolutely integrable.

In addition, there are other conditions that the function f(t) has to satisfy in order to be Fourier transformable, but we will assume that all these conditions are satisfied. In addition, it will also be assumed that

$$\int_{-\infty}^{\infty} |f(t)|^2 \, dt < \infty \qquad (1.13)$$

i.e., that the signal has finite energy.

Whenever the signal is sampled or the system is to be analysed on the digital computer, the continuous Fourier transform can no more be used. The discrete form of the Fourier transform is used so as to work on a digital computer. But while working on a digital computer the domain also no more remains infinite but converts to finite.

The discrete Fourier transform (DFT) pair, that applies to the sampled version of the continuous signals, is given by the following Eqn.

$$X(j) = \sum_{K=0}^{N-1} x(K) \, e^{-i 2\pi jK/N} \qquad (1.13)$$

$$x(K) = \frac{1}{N} \sum_{j=0}^{N-1} X(j) \, e^{i 2\pi jK/N} \qquad (1.14)$$

for $j = 0, 1, 2, \ldots\ldots\ldots\ldots N-1$ and

$K = 0, 1, 2, \ldots\ldots\ldots\ldots N-1$ and

X(j) and x(K) are in general complex. Eqn. (1.13) is a formula yielding a periodic sequence of numbers with period N.

1.1.11. Transfer Functions- The transfer function tells us how the Fourier spectrum X(v) of the input signal x(t) is modified by the passage through the linear, time-invariant system. More specifically, Y(v), the Fourier spectrum of the output signal y(t) is given as

$$Y(v) = H(v)\, X(v) \qquad (1.16)$$

where H(v) is known as the transfer function and it completely defines the linear-time-invariant system. It can be shown that the transfer function H(v) and the impulse response h(t) of the linear, time-invariant system form a Fourier transform pair.

1.2. Convolution and Deconvolution- If h(t) is the impulse response for any linear-time-invariant system, then the output is given by the convolution of the input signals with the impulse response. This is shown in the Fig.1.6.

This can be mathematically expressed as

$$y(t) = h(t) * x(t) \qquad (1.16)$$

$$= \int_{-\infty}^{\infty} x(\tau)\, h(t-\tau)\, d\tau \qquad (1.17)$$

Suppose we are given h(t) and y(t). Then it is possible to solve the inverse problem and find x(t). This process is called the inverse filtering or deconvolution. The system necessary to perform this particular operation is called the inverse filter and has 1/H(v) = G(v) as the transfer function. This can be mathematically expressed as

$$X(v) = 1/H(v) \cdot Y(v) \qquad (1.18)$$

or $x(t) = g(t) * y(t)$; where g(t) is the inverse Fourier transform of 1/H(v).

Substituting for y(t) from Eqn.(1.17) in Eqn.(1.18) we get,

$$x(t) = g(t) * h(t) * x(t) \qquad (1.19)$$

thus $$g(t) * h(t) = U_o(t) \qquad (1.20)$$

where $U_o(t)$ is unit impulse.

The recorded seismogram is the convolution of the initial source wavelet, the ground impulse response and the instrument response. A trace of reflection seismogram is composed of a great variety of waves that arrive at the surface but are not related to the event of our interest. The signal of interest is then masked by all these unwanted waves.

Let us see what happens to the marine seismograms.

1.7. Water Reverberations— In marine seismic operations, the water-air interface is a flat, strong reflector with reflection coefficient close to -1.

Consider the amplitude of the reflected and incident waves near the interface R. Let a_p be the amplitude of the incident longitudinal wave P_1, $a_{p'}$ the amplitude of the reflected longitudinal wave P_{11}, and a_{ps} the amplitude of the reflected transverse wave P_1S_1. Then

$$A_{pp} = a_{pp}/a_p \quad \text{and} \quad A_{ps} = a_{ps}/a_p \qquad (1.31)$$

These are termed as reflection coefficients and define the amplitudes of the reflected waves compared to the amplitude of the incident wave. The reflection coefficients depend in a complicated manner on the angle of incidence, and the velocities and densities in the media adjacent to the interface R. In normal incidence, a ray is perpendicular to the interface R so that = 0, the reflection coefficients takes the form as

$$A_{pp} = \frac{\rho_1 v_{p1} - \rho_2 v_{p2}}{\rho_1 v_{p1} + \rho_2 v_{p2}} \quad \text{and} \qquad (1.32)$$

$$A_{ps} = 0. \qquad (1.33)$$

where ρ_1 is the density and v_{p1} is the velocity of the first medium and ρ_2 is the density and v_{p2} is the velocity of the second media.

The product $\rho v = r$ is called the wave impedance of the medium. It is clear from Eq.(1.82) that the reflected wave forms only when

$$\rho_1 v_{p1} \neq \rho_2 v_{p2} \qquad (1.84)$$

Thus, reflected waves form at the boundaries that separate layers with different wave impedances. Such boundaries are called reflecting boundaries.

In many areas the water-bottom interface is also a strong reflector. We then have an energy trap, a non attenuating medium bounded by two strong reflecting interfaces. A pulse generated in the trap, or entering the trap from below, will be successively reflected between the two interfaces, with a time interval equal to the two-way travel time, and an amplitude decay dependent on the reflection coefficients. Because of this, valid primary reflections from depths are obscured by previously established reverberations.

The water reverberation problem was first recognized on the basis of the apparent periodicity of a suite of seismograms from the Persian Gulf[57] and treated for one-layer case. Since then ringing records have been recognized as a serious and wide spread limitation to the acquisition of valid subsurface structural information.

1.0. History of Seismic Data Processing- The field of seismic data processing has seen its most important developments in the last 35 years. Major advances have been made in the complexity and realism of the underlying mathematical models of geophysical data, in the efficiency and sophistication of the digital data processing algorithms used, and the introduction and innovative wide use of digital computers.

The first significant advance in geophysical data processing is associated with the MIT GAG Group and the related work of Robinson[43], Treitel[52], Claerbout[14] etc. Their important contributions are two fold (1) they provided fairly sophisticated models for seismic data processing in terms of random time series, and (11) they utilized for seismic data processing the then very advanced statistical filtering and smoothing algorithms of Wiener[53] etc. The contributions of the GAG Group coupled with the introduction of the digital computer in the early mid-sixties completely revolutionized seismic processing. Following the work of the GAG Group, there have been many other contributions. Among these are those of Goupillaud[20], Treitel[48] etc. on the modelling and algorithmic aspects of seismic data processing .

17

In the mid-sixties other major developments in geophysical data processing method took place. Among them are the development of the cepstral domain deconvolution by Oppenheim et. al.[12], which has been applied to geophysical data processing by Ulrych[20] and Stoffa [9,10].

1.3. Present Work:- The present study exposes the theoretical concepts and formulation of the process and examines the applicability of cepstral domain deconvolution for the estimation of the source wavelet and the transmission function for the real marine data recorded at Louisiana continental shelf by the Oil and Natural Gas Commission Offshore Seismic Exploration party. All the computer programmes to do the whole process on a digital computer were developed and tested with the above said real data set.

The second chapter deals with the theoretical aspects of the present problem. The third chapter deals with the computational considerations, procedure and the details regarding the real data set. The fourth chapter deals with the results and discussion and the fifth chapter concludes the work.

CHAPTER-IX

GENERAL DOMAIN DECONVOLUTION

Many wave forms of interest can be represented in terms of a convolution of component signal. The transmission system in the present context, can be assumed to be linear and time invariant with certain qualifications. To establish linearity we have to show that it is homogeneous and additive. The system is strictly speaking not homogeneous in the sense of section 1-1-4. However, within the elastic limit it behaves as homogeneous. For vibrations transmitted by a wave through a medium, the superposition principle may be formulated as follows i.e. the vibration at an assigned point caused by the combined action of a number of waves is equal to the sum of the vibrations caused by individual waves. Mathematically, for a linear differential equation, the sum of individual solutions will also be a solution of the equation.

The system under consideration is not time-invariant also in the strict sense, if the time scale of interest is large. But on smaller time scale, the lithology and the stratigraphy of the region under study can be assumed to be constant and the system can be assumed to be time-invariant.

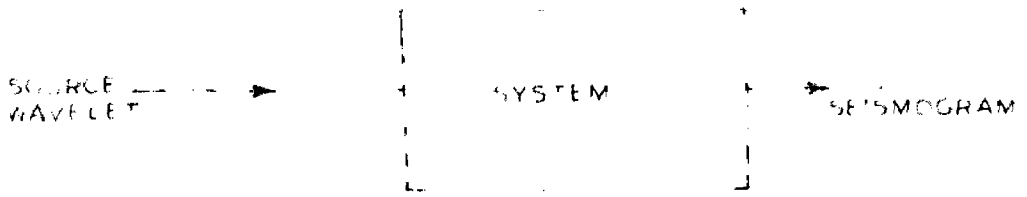

FIG. 2 1

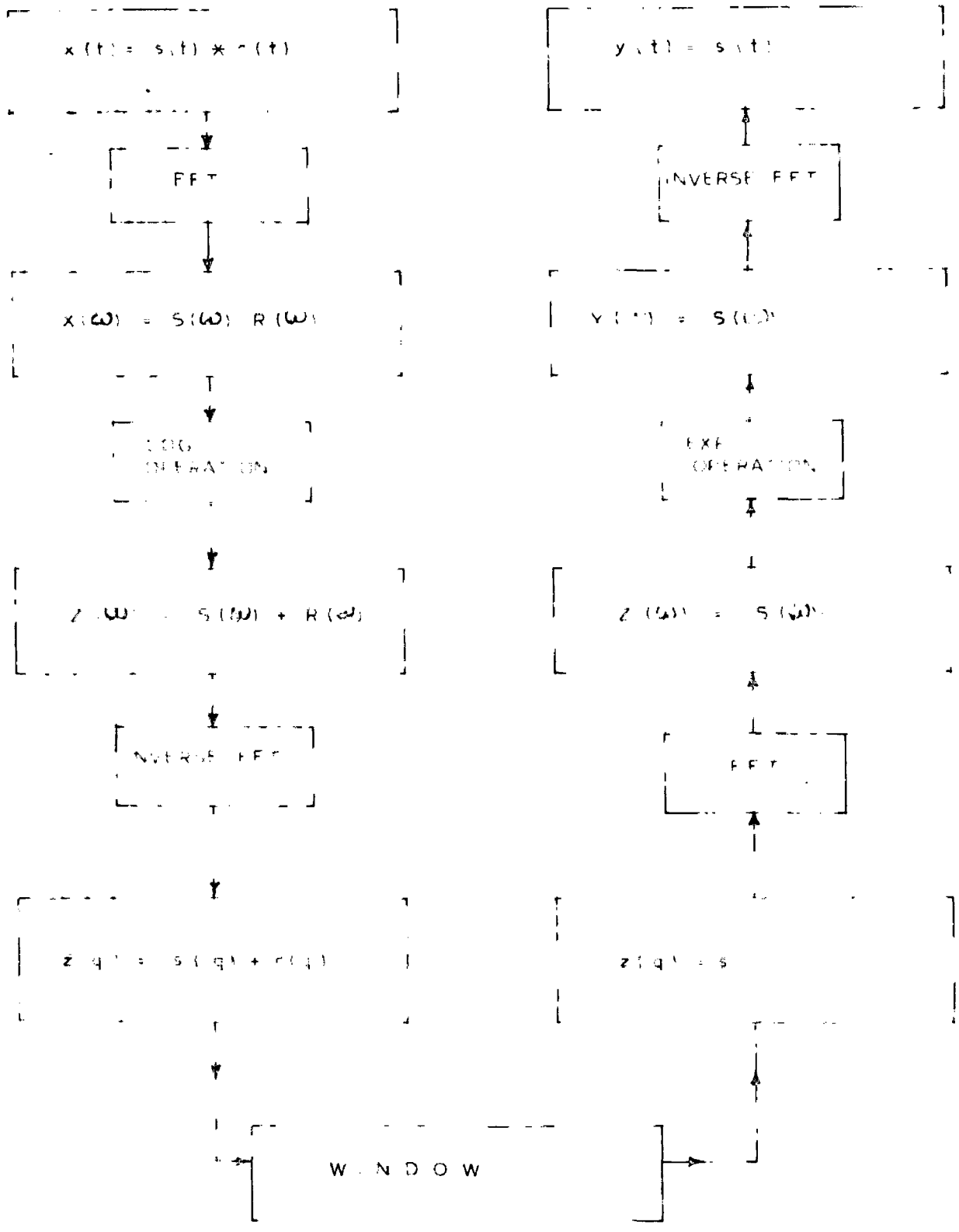

FIG 2 2 REALIZATION OF CEPSTRAL DOMAIN DECONVOLUTION USING FOURIER TRANSFORM

20

The qualifications under which the system under study is represented by convolution relationship must be kept in mind. But there is nothing unusual in the need to put qualifying clauses like these. Linearity and time-invariance of systems are conceptual abstractions and no physical system could have these attributes in the strict sense.

So what we get at the output after blasting can be represented as shown in the Fig.2.1.

Thus the seismogram which we get can be represented as the convolution of a source time function and the transmission path response as explained above. In order to separate source time function and transmission path from the convolved trace we need to have deconvolution technique. Cepstral domain deconvolution is one of the techniques which has very recently been tried (Stoffa et. al 0.D.10) for the purpose. The whole process involved in this cepstral domain deconvolution can be explained as shown as in the Fig.2.2.

2.1. Application of Cepstral Domain Deconvolution using Root Power Transform.

Fig.2.2 indicates the steps involved in the cepstral domain deconvolution. Let us examine closely how each step in the Fig.2.2 works. It can be clearly seen that there are

mainly three operations taking place.

1. The computation of the Fourier spectrum $X(\omega)$ of the time series $x(t)$, which is assumed to be given by the convolutional integral

$$x(t) = \int_{-\infty}^{\infty} c(\sigma) \cdot r(t-\sigma)\, d\sigma \qquad (2.1)$$

which in the frequency domain becomes

$$X(\omega) = C(\omega) \cdot R(\omega) \qquad (2.2)$$

where $X(\omega), C(\omega)$ and $R(\omega)$ are Fourier spectra of $x(t), c(t)$ and $r(t)$ respectively.

Eq.(2.2) can also be written as

$$X(\omega) = |X(\omega)| \cdot e^{i\phi(\omega)} \qquad (2.3)$$

where $|X(\omega)|$ and $\phi(\omega)$ are the amplitude and phase of the Fourier spectrum.

2. By the determination of the natural logarithm of the complex spectrum gives the additive superposition of the individual parts, which can be denoted by

$Z(\omega)$ which can be written as

$$Z(\omega) = \ln X(\omega) = \ln C(\omega) + \ln R(\omega) \qquad (2.4)$$

$$= \ln |X(\omega)| + i\phi(\omega) \qquad (2.6)$$

3. The computation of the inverse Fourier transform of the logarithm of the complex spectrum gives the

complex spectrum of the function x(t). The independent variable in the spectral domain is called quefrency, q, and has the dimensions of time.

$$\bar{Y}(q) = \bar{F}^{-1}(Y(\omega)) = \bar{c}(q) + \bar{x}(q) \quad (2.6)$$

Here the additivity of the single parts remains in the simplified form.

The left hand side of the Fig.2.5 indicates the operations which can be separately shown as in Fig.(2.7)

The resultant of the three operations discussed above gives us the complex spectrum which contains the phase information also. In the quefrency domain various components are separated by suitable windowing.

The right hand side of the Fig.2.5 eventually shows the reverse run of the operations. This can be shown separately as shown in the Fig.2.6. The reverse run through the first three operations as shown in the right hand side of the Fig.2.5 provides the final result of the process in the form of the filtered trace y(t).

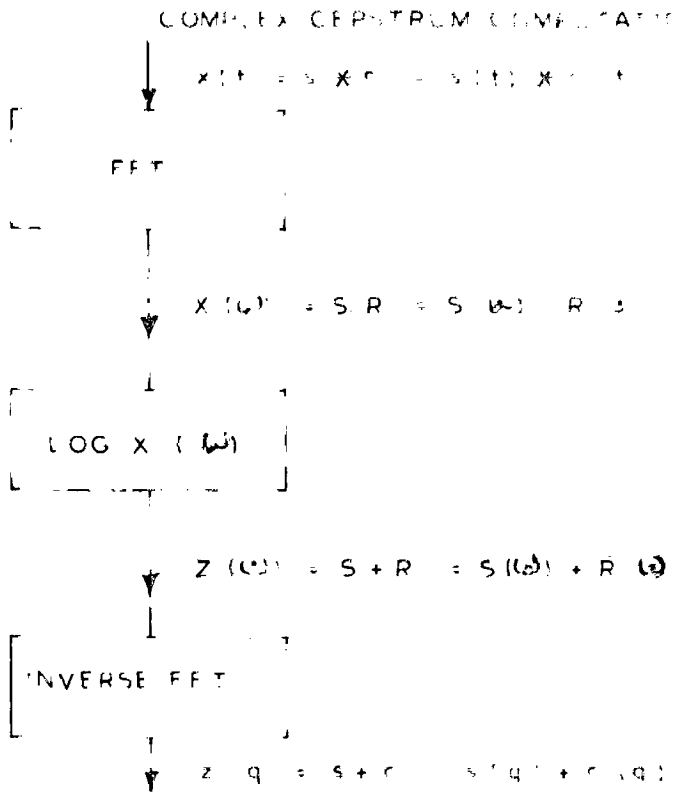

FIG 2 3 BLOCK DIAGRAM SHOWING COMPLEX CEPSTRUM COMPUTATION

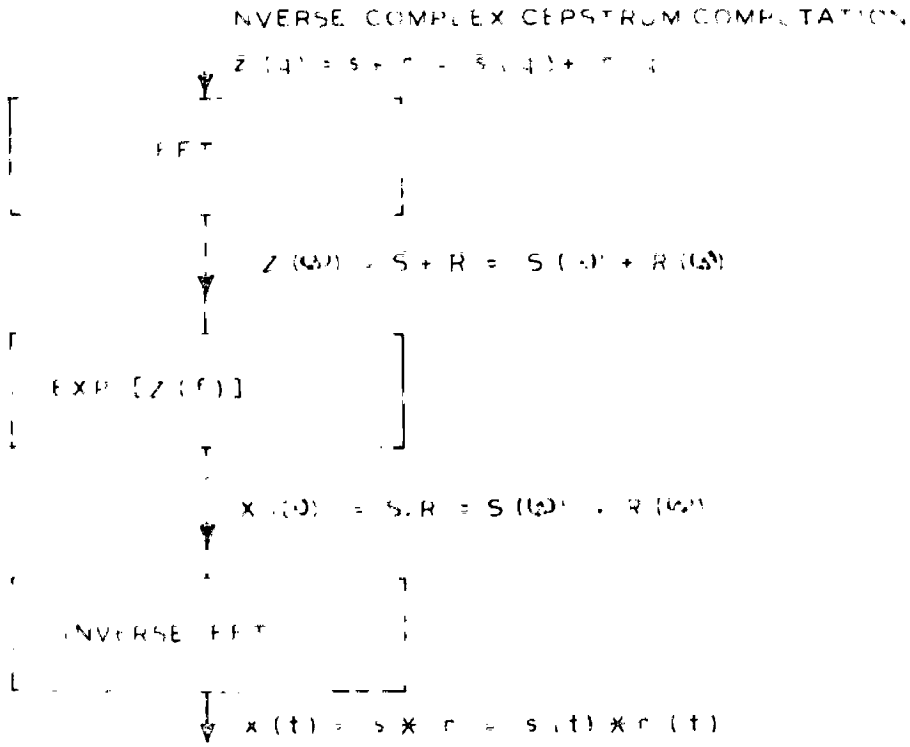

FIG 2 4 BLOCK DIAGRAM SHOWING INVERSE COMPLEX CEPSTRUM COMPUTATION

In this chapter we have seen the realization of cepstral domain deconvolution using Fourier transform. For the computational purposes we have to take into account of many factors. The next chapter actually deals with the computational considerations, the procedure of the work and also describes the data set used.

CHAPTER III

COMPUTATIONAL CONSIDERATION, PROCEDURE AND REAL DATA(NE

This chapter discusses the computational aspects of cepstral domain deconvolution, its procedure and the real marine dataset.

Before we proceed, we need some concepts from z - transform theory.

3.1. Z - Transform:- Consider a sequence of numbers x(0), x(T), x(2T), ... , x(nT), ... This sequence could, in particular, be a result of uniformly sampling a continuous waveform x(t). The z - transform of the sequence [x(nT)] defined as

$$X(z) = \sum_{n=0}^{\infty} x(nT)\, z^{-n} \qquad (3.1)$$

where z is a complex variable and it is assumed that x(nT) = 0, for negative values of n. The series in Eq.(3.1) converges for $|z| > R$ and diverges for $|z| < R$ where R is known as the radius of convergence and is the upper limit of the sequence $|x(nT)|^{1/n}$.

X(z) is an analytic function of z for $|z| > R$. Multiplying both sides of Eq.(3.1) by z^{k-1} and conducting contour integration over a path within the regions of convergence we get

$$\oint X(z)\, z^{k-1}\, dz = \oint \sum_{n=0}^{\infty} x(nT)\, z^{-n}\, z^{k-1}\, dz$$

$$= \sum_{n=0}^{\infty} x(nT) \oint z^{k-n-1}\, dz \qquad (3.2)$$

where the exchange of the order of integration and summation has been employed. According to Cauchy's theorem:

$$\oint z^{k-n-1}\, dz = \begin{cases} 2\pi j & ; \ k=n \\ 0 & ; \ k \neq n \end{cases} \qquad (3.3)$$

if the origin is surrounded by the path of integration.

Therefore

$$x(kT) = \frac{1}{2\pi j} \oint X(z)\, z^{k-1}\, dz \qquad (3.4)$$

Eq. (3.4) is the inverse z - transform relation. Usually the contour integration is performed along the unit circle.

Let X(z) and H(z) be the z - transforms of the sequences $\{x(nT)\}$ and $\{h(nT)\}$. Then it can be shown that

$$Y(z) = X(z)\, H(z) \qquad (3.5)$$

is the z - transform of the sequence $y(nT)$ where

$$y(nT) = \sum_{m=0}^{n} x(mT)\, h(nT-mT) \qquad (3.6)$$
$$= \sum_{m=0}^{n} x(nT-mT)\, h(mT)$$

This result is known as the convolution theorem. This is of fundamental importance in the study of time-

invariant linear discrete system. The sequence $[h(nT)]$ could be considered the unit sample response of the time-invariant linear discrete system and $[x(nT)]$ and $[y(nT)]$ could be considered input and output sequences respectively. Then, $[h(nT)]$ represents the sequence generated by a linear discrete system at the output when it is excited by a unit sample applied at t=0.

Let us start from the z - transform definition, i.e. Eq. (3.1)

If the z - transform is evaluated at N equispaced points on the unit circle, i.e. at

$$z = e^{j2\pi k/N}$$

where $k = 0, 1, 2, \ldots\ldots\ldots, N-1$.

Eq.(3.1) becomes

$$X\left(e^{j2\pi k/N}\right) = \sum_{n=0}^{N-1} x(nT)\, e^{-j2\pi kn/N} \qquad (3.7)$$

Now $X\left(e^{j2\pi k/N}\right)$ can be written as $X(j)$ since all other quantities in the expression are constant. Therefore

$$X(j) = \sum_{n=0}^{N-1} x(nT)\, e^{-j2\pi kn/N} \qquad (3.8)$$

This is the discrete Fourier transform defined in Eq.(1.13), in different notation. That means evaluation of the z - transform at N equispaced points

$z = e^{j2\pi k/N}$, where $k = 0, 1, \ldots, N-1$, on the unit circle, can be achieved by taking an N-sample DFT of the sequence $[x(nT)]$. Therefore, though the theoretical treatment is entirely in terms of z-transform, for computer work the computation is done in terms of DFT with the use of Fast Fourier Transform (FFT) algorithm[6], the latter can be done very effectively.

3.2. Computational considerations:- For a given function of time say $x(t)$, its Fourier transform $X(\nu)$ consists of a real part $u(\nu)$ and an imaginary part $v(\nu)$. Now we take the complex natural logarithm.

Let us take an example, $x(t)$ transforms to $X(\nu)$ where $X(\nu) = u(\nu) + jv(\nu)$ (3.9)

This can also be written in terms of amplitude and phase as given by Eq. (3.10)

$$X(\nu) = [u^2(\nu) + v^2(\nu)]^{1/2} \cdot \exp\, j \tan^{-1}\left[\frac{v(\nu)}{u(\nu)}\right] \qquad (3.10)$$

$$= A(\nu) \cdot \exp(j\phi(\nu)) \qquad (3.11)$$

The complex natural logarithm of the expression is

$$Z(\nu) = \ln[A(\nu)] + j\,\phi(\nu) \qquad (3.12)$$

One of the difficulties which we face in computing the complex spectrum is computing the proper phase curve. While u(v) and v(v) are continuous, $\tan^{-1}\left[\frac{v(v)}{u(v)}\right]$ is in general not continuous. Since the inverse tangent function is multivalued, we have to choose the branches which make it continuous. If the principal value is determined, the resulting phase curve is restricted to $-\pi < \phi \leq \pi$.

For this reason cf. al.[8,9,10] suggested an approach for computing a continuous phase curve which considers the derivative of the phase with respect to frequency.

We know that,

$$\frac{d}{dx}\left[\tan^{-1}x\right] = \frac{1}{1+x^2} \qquad (3.13)$$

If $x = v(v)/u(v)$, and $\phi(v) = \tan^{-1} x$,

then,

$$\frac{d\phi}{dw} = \frac{1}{1+\frac{v^2(w)}{u^2(w)}} \cdot \frac{d}{dw}\left[\frac{v(w)}{u(w)}\right] \qquad (3.14)$$

and

$$\frac{d}{dw}\left[\frac{v(w)}{u(w)}\right] = \frac{\left[u(w)\frac{dv(w)}{dw} - v(w)\frac{du(w)}{dw}\right]}{u^2(w)} \qquad (3.15)$$

Substituting Eq.(3.15) in Eq.(3.14), we get

30

$$\frac{d\phi}{d\omega} = \frac{1}{u^2(\omega)+v^2(\omega)}\left[u(\omega)\frac{dv(\omega)}{d\omega} - v(\omega)\frac{du(\omega)}{d\omega}\right] \quad (3.16)$$

Integration of Eq.(3.16) yields a continuous phase curve.

The derivatives dv(v)/dv and du(v)/dv can be found to desired accuracy by finding the Fourier transform of $\theta_n(t)$. The integration can also performed to the desired accuracy by using QSF (quadrature Simpson's Formula)[50]. In addition to computing a continuous phase curve, this derivative approach offers a method of removing the linear phase shift, that is the mean value of $d\phi/dv$. Determining this mean value, removing it from $d\phi/dv$ and then integrating gives the continuous zero-free phase curve in which we are interested.

A new phase unwrapping algorithm has been suggested by J. Tribolet in April 1977.[50]

Here is an adaptive numerical integration scheme that combines the information contained in both the phase derivative and the principle value of the phase, as follows: at each frequency, a set of permissible phase values is defined by adding integer multiples of 2π to the principal value of the phase. The selection of one of these values as the value of the unwrapped phase at this frequency is

31

done with the help of a phase estimate formed by numerical integration of the phase derivative with a given step interval. This step interval is changed until the phase estimate becomes arbitrarily close. Tribolet's method has been used in spectral domain deconvolution of seismic data with encouraging results[30].

But in this dissertation we used the Oppenheim et. al[3,9] phase unwrapping algorithm which has been described in section 3.2.

An important physical concept often encountered in the study of seismic waves is the concept of minimum phase.

3.3. Minimum Phase Signals- A signal x(t) such that $x(t) = 0$ for $t<0$ (3.17) is known as the causal signal. If X(w) is the Fourier transform, the requirement of causality is that all the singularities of X(s), where $s = w + j\sigma$ is a complex variable, should be in the upper half s - plane.

The signals such that their spectrum have both the poles and zeroes in the upper half s - plane are known as minimum phase signals. If the filter with transfer function H(w), the inverse filter with transfer function 1/H(w) are both to be causal, the condition is that both the poles and zeroes of the transfer function H(s) be in

the upper half s - plane. It can be noted that minimum phase signal is by definition a causal signal, but not all causal signals are minimum phase. The decomposition of a transfer function in two parts such that one has all the poles and zeroes in the upper half s - plane and the other has all the poles and zeroes in the lower half s - plane is known as spectral factorization. The function whose spectrum has all the poles and zeroes in the lower half s - plane is called a maximum phase function. Thus in a way, spectral factorization is a way of splitting the function in two portions; one is a minimum phase function and the other a maximum phase function. This splitting is achieved by writing the complex spectrum as a product. Therefore any function is a convolution of its minimum phase component and a maximum phase component.

Alternatively, minimum phase functions have some interesting properties which can be stated in terms of Hilbert transforms.

Hilbert transform- The Hilbert transform $\hat{x}(t)$ of $x(t)$ is defined as

$$\hat{x}(t) = -\frac{1}{\pi}\oint \frac{x(\tau)}{t-\tau}\, d\tau \qquad (3.10)$$

where $\oint$ denotes the integration in the Cauchy prin-

That is

$$\oint_{-\infty}^{\infty} \frac{x(\tau)}{t-\tau} d\tau = \lim_{\epsilon \to 0} \left[\int_{-\infty}^{t-\epsilon} \frac{x(\tau)}{t-\tau} d\tau + \int_{t+\epsilon}^{\infty} \frac{x(\tau)}{t-\tau} d\tau \right] \qquad (3.19)$$

The integral in Eq.(3.18) cannot be evaluated in the normal sense as the integrand has a singularity at $\tau = t$. Therefore the limiting operation indicated in Eq. (3.19) has to be conducted to avoid the difficulty.

The inverse Hilbert transform is defined as

$$x(t) = \frac{1}{\pi} \oint_{-\infty}^{\infty} \frac{x(\tau)}{t-\tau} d\tau \qquad (3.20)$$

The real and imaginary parts of the Fourier spectrum of a causal signal form a Hilbert transform pair[17]. That is,

The signal $x(t)$ can be written as

$$x(t) = x_e(t) + x_o(t) \qquad (3.21)$$

where $x_e(t)$ and $x_o(t)$ are even and odd parts of $x(t)$ respectively.

$$\text{If } x(t) \longleftrightarrow X(v), \text{ where}$$

$$X(v) = Re\, x(v) + j\, Im\, X(v) \qquad (3.22)$$

But taking Fourier transform of both sides in Eq.(3.21) we get

34

$$X(v) = X_e(v) + X_o(v) \qquad (3.23)$$

where $x_e(t) \longleftrightarrow X_e(v)$ and $x_o(t) \longleftrightarrow X_o(v)$.

Comparing Eqs.(3.20) and (3.23) in the context of the fact that the Fourier transform of an even function is real and that the Fourier transform of an odd function is imaginary, we get

$$X_e(v) = \mathrm{Re}\, X(v) \quad \text{and}$$
$$X_o(v) = \mathrm{Im}\, X(v) \qquad (3.24)$$

and now these can be represented as

$$\mathrm{Re}\, X(v) = \frac{1}{\pi} \oint \frac{\mathrm{Im}\, X(\tau)}{v - \tau} d\tau$$

$$\text{and} \qquad \mathrm{Im}\, X(v) = -\frac{1}{\pi} \oint \frac{\mathrm{Re}\, X(\tau)}{v - \tau} d\tau \qquad (3.25)$$

Thus Eq.(3.23) indicated that the real and imaginary parts of the Fourier transform of a causal function form a Hilbert transform pair.

$$\text{Let } X(v) = \mathrm{Re}\, X(v) + j\, \mathrm{Im}\, X(v) \qquad (3.26)$$

$$= A(v) \cdot e^{j\phi(v)} \qquad (3.27)$$

where $A(v)$ and $\phi(v)$ are amplitude and phase spectra then

$$\ln X(v) = \ln A(v) + j\, \phi(v) \qquad (3.28)$$

35

Thus ln A(v) and $\phi(v)$ are real and imaginary parts of ln X(v). So if ln X(v) is the spectrum of some seismic signal, then ln A(v) and $\phi(v)$ will be related as a Hilbert transform pair and therefore the phase spectrum $\phi(v)$ would be fully obtainable from the amplitude spectrum A(v). If ln X(v) is to be the spectrum of some seismic signal ln X(z) must have all its poles in the upper half z - plane. But the poles of ln X(z) are the poles of X(z) as well as the zeroes of X(z). Thus the requirement is that the poles as well as the zeroes of X(z) must lie in the upper half of the z - plane. Thus if both the poles as well as the zeroes of X(z) lie in the upper half z - plane, i.e. if x(t) is a minimum phase signal, then not only is there a Hilbert transform relationship between Re X(v) and Im X(v) but also between the ln A(v) and $\phi(v)$.

In marine seismic exploration the signals which we get are in the mixed phase. The mixed phase sequence may be made into a minimum phase sequence by means of exponential weighting.

36

3.4. Hilbert's Eq. (3.29)

$$X(z) = \sum_{n=-\infty}^{\infty} x(nT)\, z^{-n} \qquad (3.29)$$

we have transformed a real time function into its z - transform $X(z)$, which exists throughout the complex z - plane.

$$\bar{X}(z) = \ln X(z)$$
$$= \ln |X(z)| + j \arg |X(z)| \qquad (3.30)$$

$$\bar{x}(n) = \frac{1}{2\pi j} \oint \bar{X}(z)\, z^{n-1}\, dz \qquad (3.31)$$

where $n = 0, \pm 1, \pm 2, \ldots\ldots\ldots\ldots$

Eq. (3.31) gives the complex cepstrum for discrete functions of unit sample interval. Thus $\bar{x}(n)$ is a function of the particular contour. In computing the complex cepstrum, we use the discrete Fourier transform for real frequencies in place of the z - transform, thus restricting the contour to the unit circle ($\sigma = 0$). However if we replace the sequence $[x(nT)]$ by $[x(nT)\, a^{-nT}]$, where $0<a<1$, we have effectively moved our integration contour to a circle of radius a^{σ} where

$$\sigma = -\ln a \qquad (3.32)$$

since $a < 1, \sigma$ is positive, and $a^{-\sigma nT}$ is an exponentially decaying function. The three steps involved in the reverse procedure for returning to the time domain are

37

$$X(z) = \sum_{n=-\infty}^{\infty} x(n)\, z^{-n} \qquad (3.33)$$

$$X(z) = \exp\left[\hat{X}(z)\right] \qquad (3.34)$$

$$x(n) = \frac{1}{2\pi j} \oint \hat{X}(z)\, z^{n-1}\, dz \qquad (3.35)$$

In returning to the time domain via Eqs. (3.33), (3.34), (3.35) ; we should unweight the result by α^{-n}. In the DFT, since we are confined to evaluating $\hat{X}(z)$ around the unit circle, we can consider that the effect of weighting is to move the poles and zeroes of $\hat{X}(z)$ radially inward by the factor α and unweighting with the inverse function restores them to their original location.

In the present work, we have chosen the value of 'α' as $\alpha = 0.990$, which gave favourable results which will be described in the next chapter. This value was suggested by Stoffa et.al.[9,9,10].

3.5. Procedure:- As we have shown in Fig.(3.2) by a block diagram the essential steps in the cepstral domain deconvolution are as follows:

1. We are having the marine seismic real data. Digitize the data with the sampling interval of 4 milli seconds to a get a discrete sequence.
2. Weight this input sequence by a factor $a^{|k|}$ where $a = 0.993$.
3. Take the forward Fourier transform of the weighted discrete input.
4. Take the complex natural logarithm of the Fourier transformed output.
5. Now take the inverse Fourier transform of the above out put.

This completes the computation of the complex cepstrum.

With imaginary input as zero the discrete Fourier transform was computed. The output was converted into polar form. Real part for the next operation was obtained by taking natural logarithm of the amplitude in the polar representation. Now a continuous, ramp free phase was computed with the help of Eq.(3.6).

This actually forms the imaginary part of $\ln X(\nu)$. Now with the above mentioned real and imaginary inputs the inverse Fourier transform was computed. This gives us the complex cepstrum.

The next step is windowing of the cepstrum data to recover the source time function and the transmission response.

The last step in the cepstral domain deconvolution is the recovery of the source wavelet and the transmission response. This is achieved by subjecting the output after windowing to the inverse complex cepstrum process. Finally the unweighting is done by the very same factor by which the input was weighted initially.

L1 c

2.6. Data for Analysis- The dataset used in the dissertation was collected on board on the western coast of India, namely Saurashtra Continental Shelf by the field party of Oil and Natural Gas Commission, during the offshore seismic survey in 1976 - 77.

The seismic recording system used was DFS IV, a digital recording system. The profile runs in the North - South direction which is roughly 200 - 250 kms. from the coast. The general water depth in these areas varies from 80 mtrs to 100 mtrs. The recording system used the recording frequencies as - high cut - 80 cycles/sec and low cut - zero.

The recording was done in 48 fold and 48 channels whose record length was of 6 secs. The group interval of the geophones were 50 mtrs. whereas the shot interval was 50 mtrs. The initial offset was 270 mtrs. The geophones were kept 10 mtrs below the surface of the water. The energy source was Air Guns and for each firing used an array of 6 Guns. The air-gun array was kept 6 mtrs. below the surface of the water. The digital recording was done with sampling interval of 4 milliseconds.

using the real dataset thus obtained we carried out the cepstral domain deconvolution. The next chapter deals with the results and discussion of this.

CHAPTER IV

RESULTS AND DISCUSSION

The cepstral domain deconvolution technique was tested on the marine seismic real data.

Fig.4.1. shows the complex cepstrum obtained using the above technique. This is plotted on a linear scale; i.e. we have plotted the sample numbers on abscissa and the cepstral amplitude on ordinate. The cepstrum has significant amplitude only up to the 10th sample and beyond it , it has only small variation which does not show up on the scale chosen. The complex cepstrum obtained is the addition of the complex cepstra of the source wavelet and the reflector series respectively.

A careful look at the complex cepstrum indicates that the behaviour is oscillatory in the range of small sample numbers showing both positive and negative excursions. After the fifth sample this oscillatory behaviour could be said to be over and then upto about twentieth sample the cepstrum continue to have only positive excursions and beyond that the cepstrum amplitudes are negligibly small. Of course, the positive excursion between the samples 5-8 could have been considered as part of the original oscillatory behaviour in continuation of the previous negative excursion. But this is, in any case, an individual's

judgement as the cepstrum does not separate in two distinct parts with nonoverlapping characters. So we have assumed that the part upto sample 6 could be attributed to the source wavelet and the subsequent variation to the transmission response function. It must be admitted, however, that there is some arbitrariness about the window size, which indirectly means that the cepstral domain separation of the source wavelet and transmission response function is not fully satisfactory.

The Fig.4.2 shows the recovered weighted source wavelet and the Fig.4.3 shows the recovered unweighted source wavelet. The recovered source wavelet has been plotted on a semi-log paper because of the very high amplitudes. It is possible to show only unipolar variation on a semi-log paper whereas we have to plot bipolar variation. This is achieved by placing two semi-log graphs edge to edge, one indicating + ve excursions and another indicating - ve excursions. The middle portion between -10^0 to 10^0 could be obtained by interpolation. The source wavelet contribution starts from 32nd sample and ends at 62nd sample. The duration of the source wavelet is 0.3 seconds (=300 samples). The source wavelet which we get is shifted from the origin.

A plausible explanation of this shift could be as follows. Ideally, it is assumed that the cepstrum $h_c(q)$ of the recorded seismogram has two components $h_0(q)$ and $h_p(q)$ which are cepstra of the source wavelet and the

transmission response function respectively. As stated above, $h_D(q)$ and $h_P(q)$ cannot really be separated by windowing. As a result, by windowing we get only

$$h_{D\ est}(q) = h_D(q) + h_{F\ res}(q) \qquad (4.1)$$

where $h_{D\ est}(q)$ and $h_{F\ res}(q)$ are our estimate of $h_D(q)$ and the residual part of $h_P(q)$ that is superimposed on $h_D(q)$, respectively. During the reverse passage we get the following.

(a) after Fourier transformations

$$\ln S_{est}(v) = \ln S(v) + \ln R_{res}(v) \qquad (4.2)$$

(b) after exponentiations

$$S_{est}(v) = L(v)\, R_{res}(v) \qquad (4.3)$$

Thus the estimated spectrum of $s(t)$ is the true spectrum of $s(t)$, multiplied by a factor $R_{res}(v)$ which is the effect of the contamination of the spectrum of $s(t)$ by that of $r(t)$. In general $R_{res}(v)$ will be complex, having both magnitude and phase-part. If the phase part has a linear phase component, its effect would be to shift $s(t)$ away from the time origin. By symmetry, it has to argued that the spectrum of $r(t)$ cannot be completely separated by windows and would therefore be contaminated by the spectrum of $s(t)$ and hence $r(t)$ also might be shifted away from the time origin. There of course are

effects other than just this shift. For example from Eq.(4.3) it follows that the estimated $s(t)$ is the convolution of true $s(t)$ with the inverse Fourier transform of $R_{pp}(v)$.

The recovered transmission function is shown in the Fig.4.6. Here also we have used bipolar semi-log plotting as described above.

Let us consider a case where there are a water - air and subsurface - water interfaces as shown in Fig.4.6. Consider that water is a non-dispersive medium for the time being. Fig.4.7 shows that when an impulse source is given we get the reflections at times $t_n, n = 1, 2, 3, \ldots\ldots\ldots$ reaching the receiver. It can be easily seen that $t_n = 2nx/v$ (4.4)

With the given values of the reflection coefficients (which are assumed for the illustrative purpose only) the magnitudes of the impulses reaching the receiver at $t_n = 2nx/v$ can be calculated and they are shown in Fig.4.8. Thus we get an alternating sequence of impulses with decreasing magnitudes.

Here we are getting impulses at times $t1, t2, t3, \ldots$ etc. where as in the actual case instead of getting these impulses we get broad alternating pulse which is as shown in Fig.4.9. This means that the water

is not a non-dispersive medium. If water is assumed to be dispersive various frequency components in the impulse excitation will travel at different velocities, the reflection coefficients will also be different for different frequency components as follows from Eq. 1.22. Thus arrival times t_n would be different for different frequency components of the impulse and so would be the returned amplitudes at those instances. Thus instead of every impulse, we should expect to get a broadened peak. This then explains the nature of the transmission response function of Fig. (4.6) except that the second negative peak should have had much lesser amplitude. This discrepancy could plausibly be because of the dielectric effect described in Eq. (4.3).

As we have already argued, the whole transmission response function could have been distorted by convolution with the inverse Fourier transform of $H_{FCC}(\nu)$. As a part of this effect, in particular it could have been shifted away from the time-origin. Therefore we would base all our calculations not on absolute values of t_n but on the differences $t_n - t_{n-1}$. These values are seen to be (103, 80, 80) $\times$ 4 n.sec. respectively for n=2,3,4. Thus on an average, we have as a rough estimate

$$t_n - t_{n-1} = 2x/v = 91.66 \times 4 \text{ n.sec.}$$
$$= 0.3666 \text{ sec.} \qquad (4.5)$$

Thus from our results we can roughly estimate the source wavelet duration to be 0.02 secs. and the two-way travel time of the wave to be 0.3333 secs. As already emphasized by Futterman[11], for the temporal domain deconvolution to work satisfactorily, the source wavelet duration should be small in comparison to the two-way travel time of the wave. It is obvious that this requirement was not satisfied in our case. This in turn meant that the choice of the window was not simple in our case and thus the contamination of $h_0(t)$ by $h_{2\pi}(t)$ and that of $h_{2\pi}(t)$ by h_0 was not negligible.

Let us consider that the source wavelet is convolved with the reflector series.

$$r(t) = s(t) * x(t) \qquad (4.6)$$

$$\downarrow \text{FFT}$$

$$R(\nu) = S(\nu) \cdot X(\nu) \qquad (4.7)$$

$$\downarrow \text{LOG}$$

$$\overline{R}(\nu) = \overline{S}(\nu) + \overline{X}(\nu) \qquad (4.8)$$

$$\downarrow \text{INVERSE FFT}$$

$$h_m(t) = h_0(t) + h_{2\pi}(t) \qquad (4.9)$$

Now let us define

$$\hat{h}_0(t) = h_m(t)\,[u(t+T) - u(t-T)] \qquad (4.10)$$

$$\downarrow \text{FFT}$$

$$S(\nu) = h_m(\nu) * \left[2T \frac{\sin 2\pi\nu T}{2\pi\nu T}\right] \qquad (4.11)$$

Now taking the Exponential form we get

$$X(\nu) = o^{h_x(\nu)*[\pi \frac{\sin \pi\nu}{\pi\nu}]} \qquad (4.22)$$

INVERSE FT

$$o(t) = \frac{1}{2\pi}\int_{-\infty}^{\infty} o^{h_x(\nu)*[\pi \frac{\sin \pi\nu}{\pi\nu}]} e^{j\omega t} d\omega \qquad (4.23)$$

The question is when is $\hat{o}(t) = o(t)$?

This is only when

$$h_x(q) = h_x(0), \quad |q| < \tau \qquad (4.24)$$

$$h_x(q) = h_x(q)_0 \quad |q| > \tau \qquad (4.25)$$

This is possible only and only if

$$h_x(q) = 0_0 \qquad |q| > \tau \qquad (4.26)$$

$$h_x(q) = 0_0 \qquad |q| < \tau \qquad (4.27)$$

What we get is not $o(t)$ but $o(t)_0$

$$\hat{o}(t) = \frac{1}{2\pi}\int_{-\infty}^{\infty} e^{j\omega t} o^{h_x(\nu)*[\pi \sin \pi\nu/\pi\nu]} d\omega \qquad (4.28)$$

$$= \frac{1}{2\pi}\int_{-\infty}^{\infty} \left\{ \int k_x(q)\, e^{j\omega q} dq \right\} * \left[2T \frac{\sin \omega T}{\omega T}\right] e^{j\omega t} d\omega \qquad (4.19)$$

$$= \frac{1}{2\pi}\int_{-\infty}^{\infty} \left\{ F.T\left[k_x(q)\right] * \left[2T \frac{\sin \omega T}{\omega T}\right] e^{j\omega t} d\omega \right. \qquad (4.20)$$

$$= \frac{1}{2\pi} \int_{-\infty}^{\infty} e^{[\ln X(w)] * [2T \sin wT/wT]} \; e^{jwt} \; dw \qquad (4.21)$$

$$= \frac{1}{2\pi} \int_{-\infty}^{\infty} e^{[\ln S(w) + \ln R(w)] * [2T \sin wT/wT]} \cdot e^{jwt} \; dw \qquad (4.22)$$

$$= \frac{1}{2\pi} \int_{-\infty}^{\infty} e^{[\ln S(w)] * [2T \sin wT/wT]} \cdot e^{[\ln X(w)] * [2T \sin wT/wT]} \cdot e^{jwt} \; dw \qquad (4.23)$$

If $e^{[\ln R(w)] * [2T \sin wT/wT]} = 1$

i.e. if $R(w) = 1$;

i.e. if $r(t) = \delta(t)$.

Now Eq.(4.23) becomes;

$$s(t) = \frac{1}{2\pi} \int_{-\infty}^{\infty} e^{[\ln S(w)] * [2T \sin wT/wT]} \cdot e^{jwt} \; dw \qquad (4.24)$$

Further as $[2T \sin wT/wT] \longrightarrow \delta(w)$;

i.e. if $T \longrightarrow \infty$.

we would get

$$\hat{c}(t) = \frac{\partial}{\partial \tau} \int_{-\infty}^{\infty} [\ln S(\nu)] * S(\nu) \cdot e^{j\nu t}\, d\nu \qquad (4.25)$$

$$= \frac{\partial}{\partial \tau} \int_{-\infty}^{\infty} e^{\ln S(\nu)}\, e^{j\nu t}\, d\nu \qquad (4.26)$$

$$= \frac{\partial}{\partial \tau} \int_{-\infty}^{\infty} S(\nu)\, e^{j\nu t}\, d\nu \qquad (4.27)$$

$$= c(t) \qquad (4.28)$$

By symmetry $r(t) = r(t)$;

$$\text{iff } c(t) = s(t) \text{ and } \tau \longrightarrow \infty$$

In practice, the recorded seismogram has an additive noise component also. This can be represented as:

$$x(t) = c(t) * r(t) + n(t) \qquad (4.29)$$

where $n(t)$ is the additive noise component. After taking the Fourier transform Eq.(4.29) becomes

$$X(\nu) = S(\nu)\, R(\nu) + N(\nu)$$

$$= S(\nu)\, R(\nu) \left[1 + \frac{N(\nu)}{S(\nu)\, R(\nu)}\right] \qquad (4.30)$$

After taking the logarithm, we get

$$\ln X(\nu) = \ln S(\nu) + \ln R(\nu) + \ln\left[1 + \frac{N(\nu)}{S(\nu)\, R(\nu)}\right] \qquad (4.31)$$

Let us assume that the spectral energy in the noise is small so that the last term can be expanded as

$$\ln\left[1 + N(v)/S(v)H(v)\right] = N(v)\,P(v)\,Q(v) - \frac{1}{2}\left|N(v)P(v)Q(v)\right|^2 + \frac{1}{3}\left|N(v)P(v)Q(v)\right|^3 - \cdots\cdots\cdots \qquad (4.32)$$

where $P(v) = 1/S(v)$ and $Q(v) = 1/H(v)$

Then taking the inverse Fourier transform we get:

$$ln(q) = ln_0(q) + ln_r(q) + \left[g(q) - \frac{1}{2}\,g(q)*g(q) + \frac{1}{3}\,g(q)*g(q)*g(q) - \cdots\cdots\cdots\right] \qquad (4.33)$$

where $ln(q)$, $ln_0(q)$ and $ln_r(q)$ are spectra of $n(t)$, $o(t)$ and $r(t)$ respectively and $g(q)$ is the inverse Fourier transform of $N(v)P(v)Q(v)$. In particular,

$$g(q) = n(q)*p(q)*q(q) \qquad (4.34)$$

where $p(q)$ and $q(q)$ are inverse Fourier transforms of $P(v) = 1/S(v)$ and $Q(v) = 1/H(v)$ respectively. Note that $n(t)$, the noise occupies the entire range of time.

Furthermore, the quefrency duration of $g(q)$ would be larger than that of $n(q)$ alone, as convolution is a duration - expanding operation. Further, the term $g(q)*g(q)$ will have twice the quefrency duration as that of $g(q)$, the term $g(q)*g(q)*g(q)$ will have twice the quefrency duration as that of $g(q)$ and so on. Thus the terms in curly brackets in Eq.(4.33) have a very large quefrency duration so that it could be assumed to occupy the whole range of quefrencies. Thus even if the cepstra $k_0(q)$ and $k_r(q)$ were to be non-overlapping in quefrency in the absence of noise $n(t)$, so that they could be separated by windowing, the clear quefrency separation between them will be masked by the effect of noise. The choice of a window duration thus is made difficult by noise.

The noise has another effect too. Let us try to obtain $\hat{k}_0(q)$, the estimate of $k_0(q)$ by multiplying $k_m(q)$ by the window $v(q)$. Then,

$$\hat{k}_0(q) = k_m(q)\, v(q)$$

$$= k_0(q)\, v(q) + k_r(q)\, v(q) + \left[g(q) - \frac{1}{2} g(q)\, g(q) + \frac{1}{3} g(q)\, g(q)\, g(q)\right] v(q)$$

(4.36)

The $k_r(q)v(q)$ term was written as k_r $e_0(q)$ in Eq.(4.1) earlier and its effect already has been discussed.

The effect of noise is more difficult to analyse, because it depends on what the inverse cepstrum of

$$d(q) = [\, g(q) - \tfrac{1}{2}\, g(q)*g(q) + \tfrac{1}{3}\, g(q)*g(q)*g(q) - \ldots\ldots\ldots\ldots\ldots\ldots\,] \; v(q) \text{ is.} \qquad (4.30)$$

But one thing that can be concluded is that the effect of noise is not independent of what the source wavelet and the transmission response function are. They may term in deciding the effect of noise is $d(q)$ which depends on $g(q)$ which is $n(q)*p(q)*q(q)$ where $p(q)$ and $q(q)$ are Fourier inverse transforms of $P(v) = 1/B(v)$ and $Q(v) = 1/A(v)$. Thus the effect of the additive noise term on the cepstral domain deconvolution is very complex.

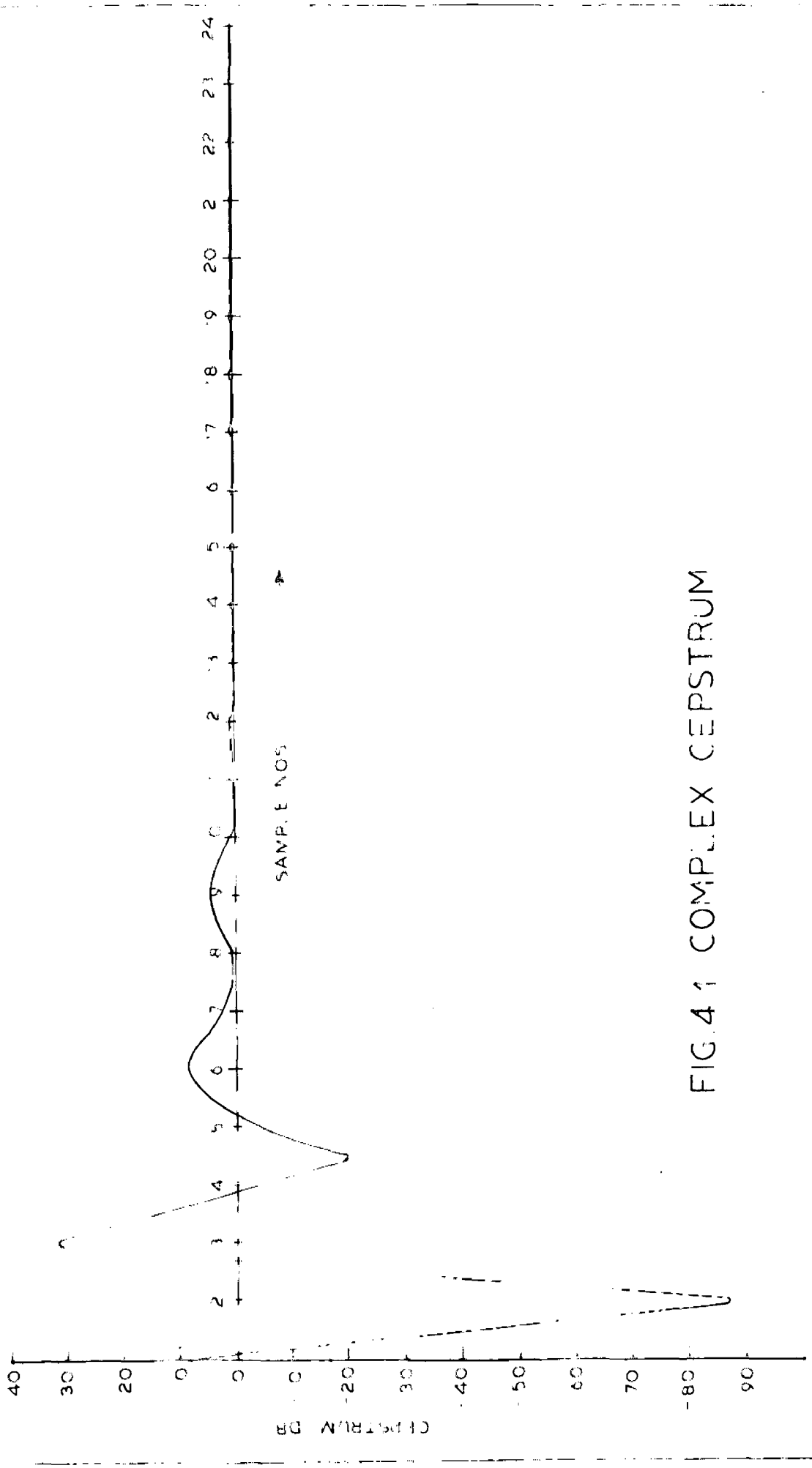

FIG.4.1 COMPLEX CEPSTRUM

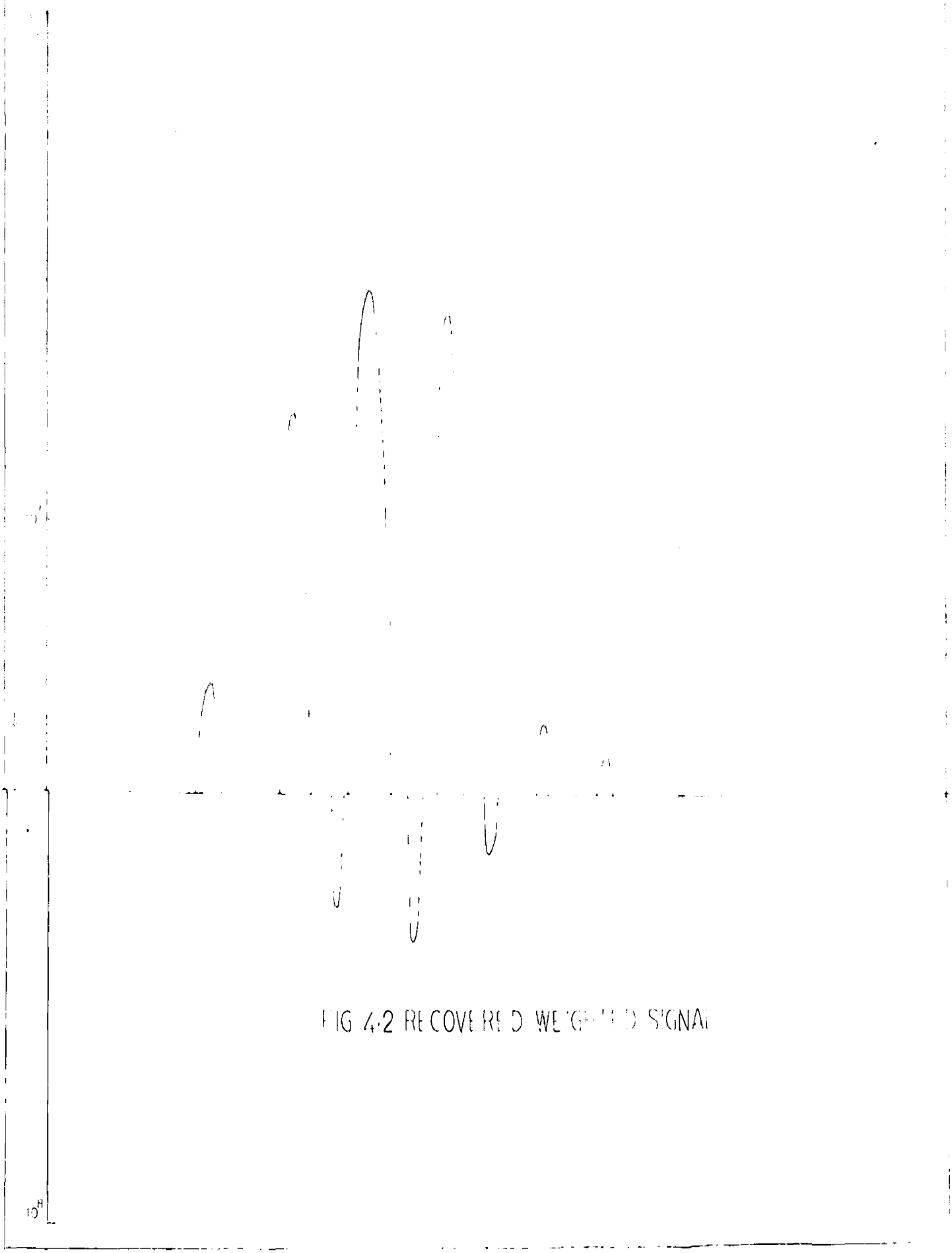

FIG 4·2 RECOVERED WEIGHTED SIGNAL

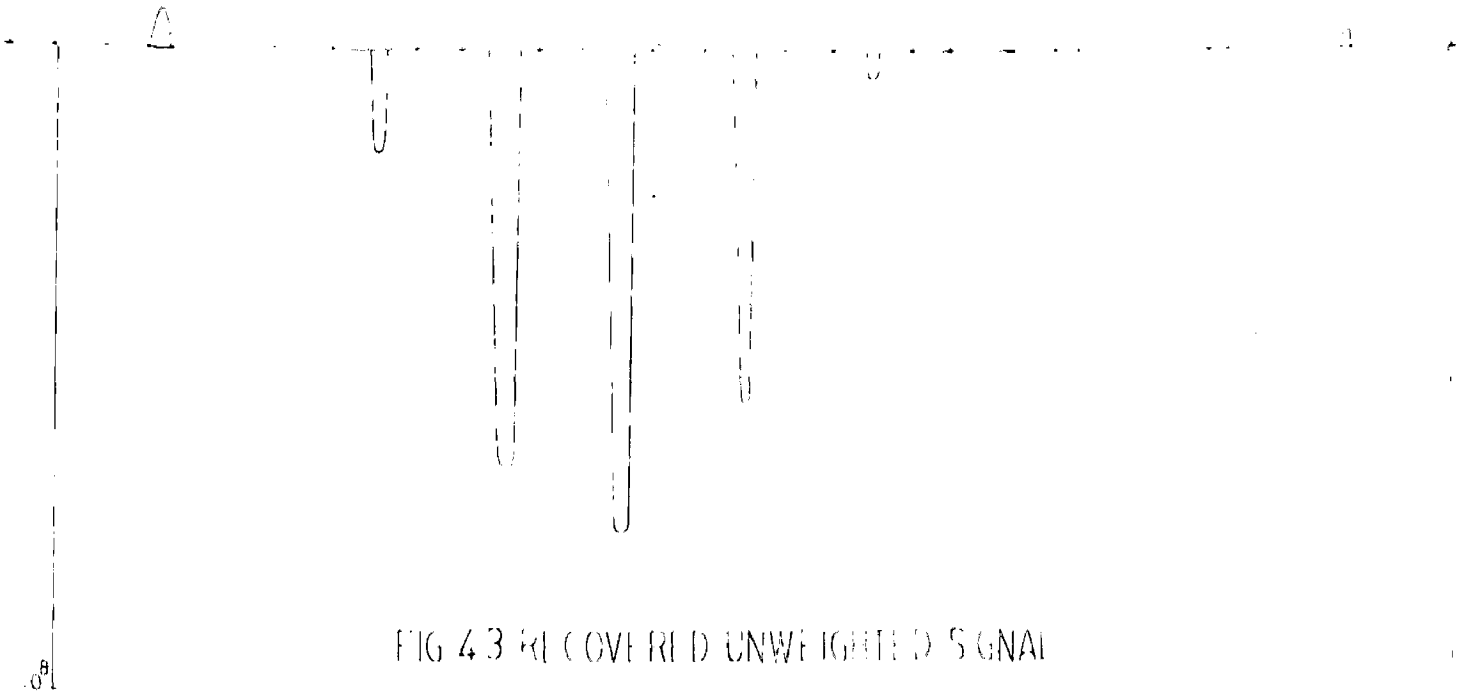

FIG 4.3 RECOVERED UNWEIGHTED SIGNAL

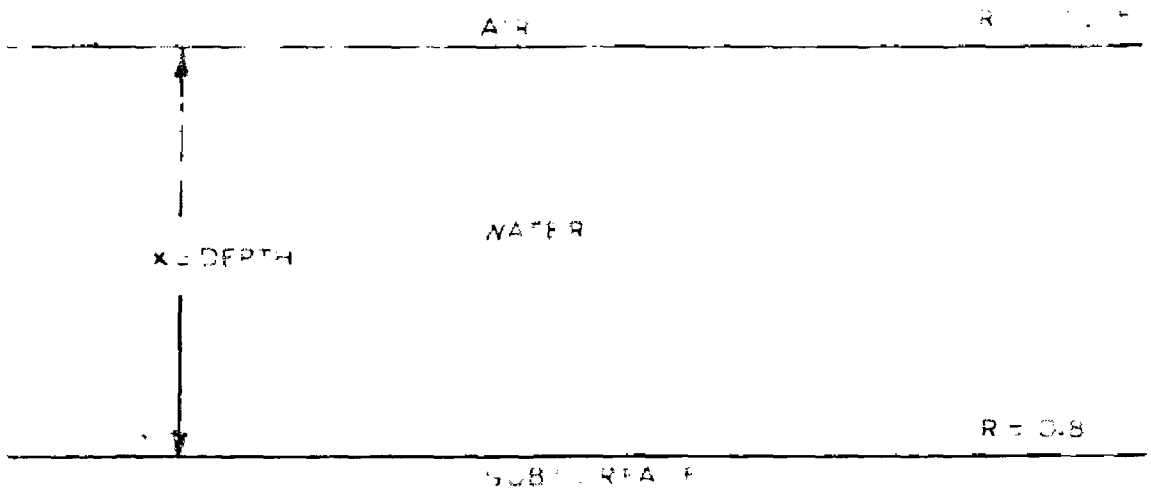

FIG. 4.6 – SCHEMATIC DIAGRAM OF A WATER LAYER BOUNDED ABOVE BY A PERFECT REFLECTOR R_0 AND BELOW BY A HARD BOTTOM OF REFLECTION COEFFICIENT R.

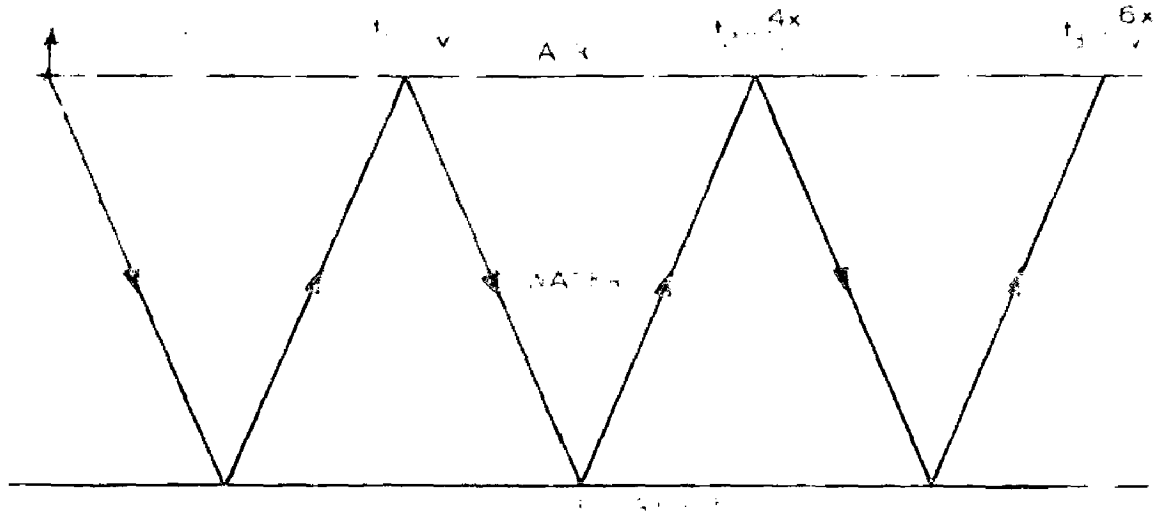

FIG. 4.7 – REFLECTION RAY PATH.

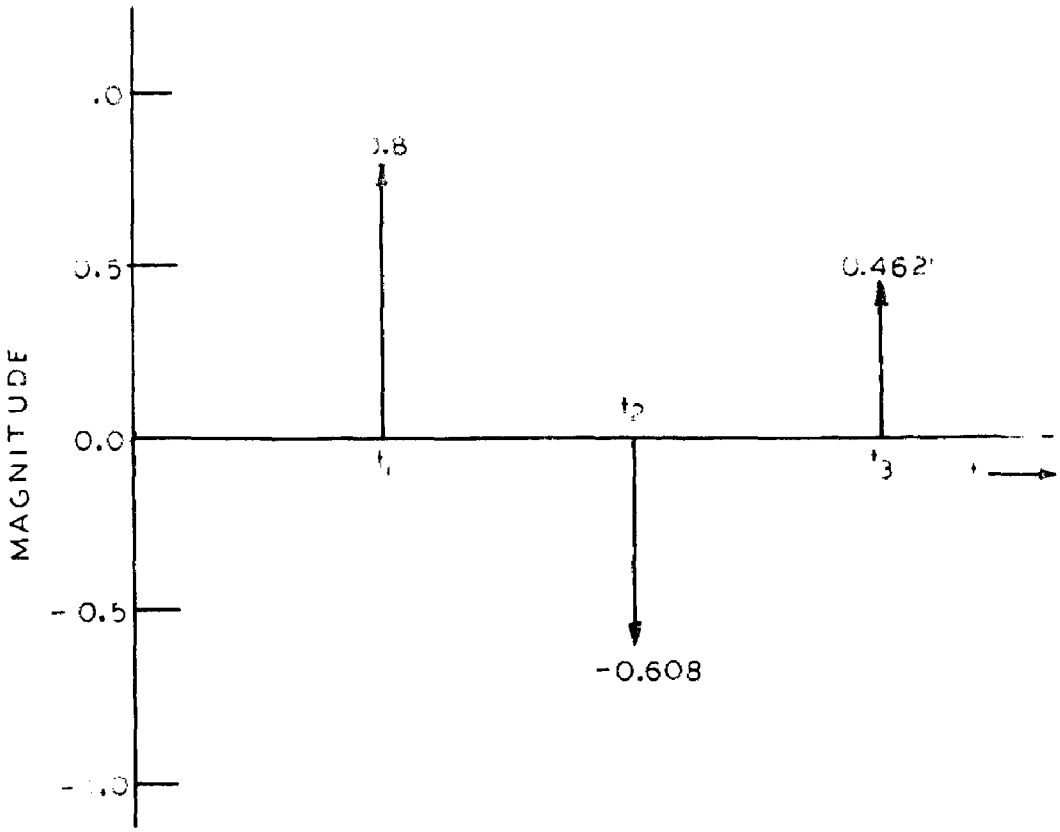

FIG.4.8 - DECAYING IMPULSES.

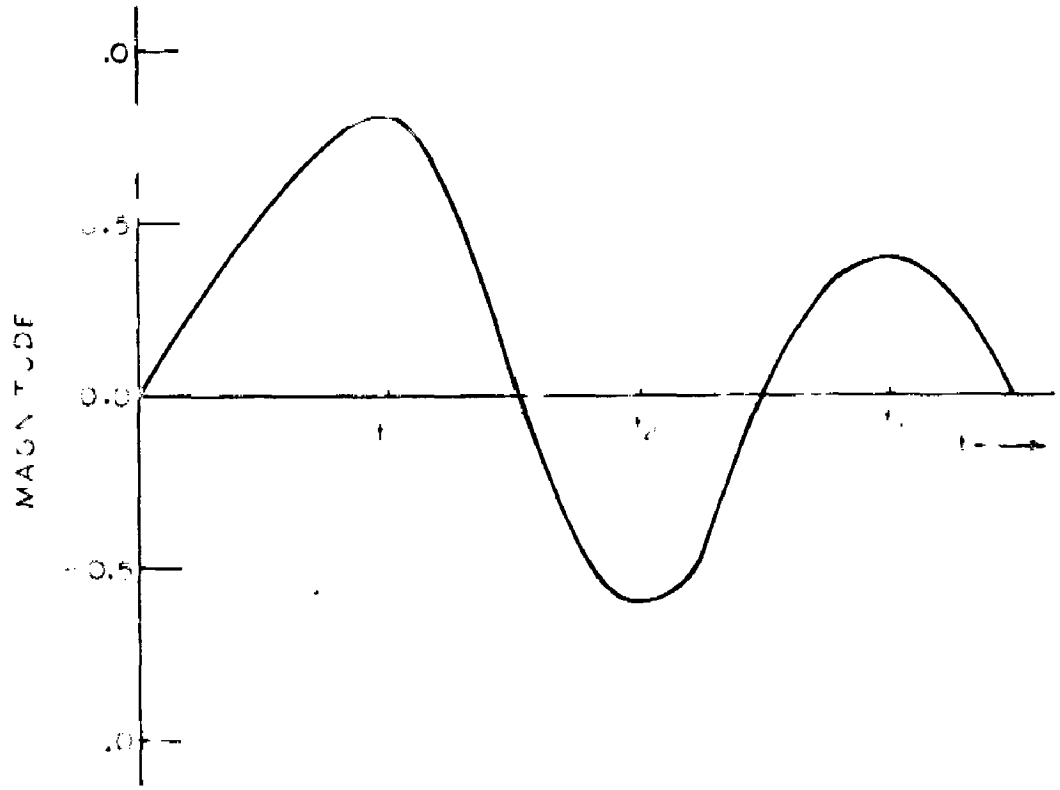

FIG.4.9 - BOARD ALTERNATING PULSE .

61

CHAPTER V

CONCLUSION

In this dissertation we have applied the Cepstral Domain Deconvolution technique to recover the source wavelet and the transmission response from the noise seismogram. We were able to separate the source wavelet and the transmission response. From our results we calculated the source wavelet duration to be 0.03 secs. and the travel time of the wave from the sea surface to the water-subsurface to be 0.0004 secs. For the Cepstral Domain Deconvolution to work satisfactorily the source wavelet duration should be small in comparison to the two-way travel time of the wave. It is clear that this requirement was not satisfied in our case. This in turn means that the choice of the window was not simple in our case and thus the contaminations of ln(q) by ln rec(q) and that of ln (q) by ln rec (q) were not negligible. The future work in this field can be done for designing suitable windows instead of the rectangular window which can minimize the contaminations which are described above.

52

The crustal transmission response curves can be used for inferring the subsurface if we have a knowledge of the velocity using Eq.(4.4).

- . -

63

```
C      MAIN
C      CEPSTRAL DOMAIN DECONVOLUTION OF MARINE SEISMIC REAL DATA ASKNAIR
       DIMENSION XR(1024),XI(1024),XRW(1024),XIW(1024),AMPR(1024)
       DIMENSION CEP(1024),G(1024),S(1024),AXR(1024),AXI(1024)
       DIMENSION BXR(1024),BXI(1024),H(1024)
       COMMON A,N,MM,DOT,BLANK,LX,DT
       READ 10,N,MM,A,DOT,BLANK,DT,IN
       PRINT 10,N,MM,A,DOT,BLANK,DT,IN
   10  FORMAT(2I4,F6.3,2A1,F6.4,I2)
       LX=2**N
       DO6NN=1,LX
       XRW(NN)=0.
       XIW(NN)=0.
       XR(NN)=0.
    6  XI(NN)=0.
       READ 14,(XR(I),I=1,MM)
   14  FORMAT(7E11.5)
C      NOW WE ARE WEIGHTING THE FUNCTION
       DO15 I=1,LX
       B=I-1
       Y=A**B
   15  XRW(I)=XR(I)*Y
       WRITE(6,30)
   30  FORMAT(1X,/25X, TIME-SERIES ,25X, WEIGHTED TIME-SERIES /)
       CALL PLOT (XR,XRW,1,500)
       DO29I=1,LX
   29  G(I)=XRW(I)
       CALL FFT (XRW,XIW,-1.)
C      NOW WE ARE MULTIPLYING THE SIGNAL BY T
       DO9I=1,LX
       T=I-1
    9  XR(I)=T*G(I)*DT
C      NOW WE ARE COMPUTING THE PHASE
       CALL FFT (XR,XI,-1.)
       AVPH=0.
       LY=LX/2+1
       DO4I=1,LY
       VD=XRW(I)*XRW(I)+XIW(I)*XIW(I)
       XR(I)=-(XRW(I)*XR(I)+XIW(I)*XI(I))/VD
       AVPH=AVPH+XR(I)
```

APPENDIX I

COMPUTER PROGRAMME FOR CEPSTRAL DOMAIN DECONVOLUTION

63

```
C     MAIN
C     CEPSTRAL DOMAIN DECONVOLUTION OF MARINE SEISMIC REAL DATA ASKNAIR
      DIMENSION XR(1024),XI(1024),XRW(1024),XIW(1024),AMPR(1024)
      DIMENSION CEP(1024),G(1024),S(1024),AXR(1024),AXI(1024)
      DIMENSION BXR(1024),BXI(1024),H(1(24)
      COMMON A,N,MM,DOT,BLANK,LX,DT
      READ 10,N,MM,A,DOT,BLANK,DT,IN
      PRINT 10,N,MM,A,DOT,BLANK,DT,IN
   10 FORMAT(2I4,F6.3,2A1,F6.4,I2)
      LX=2**N
      DO6NN=1,LX
      XRW(NN)=0.
      XIW(NN)=0.
      XR(NN)=0.
    6 XI(NN)=0.
      READ 14,(XR(I),I=1,MM)
   14 FORMAT(7E11.5)
C     NOW WE ARE WEIGHTING THE FUNCTION
      DO15 I=1,LX
      U=I-1
      Y=A**U
   15 XRW(I)=XR(I)*Y
      WRITE(6,90)
   90 FORMAT(1X,/29X, TIME-SERIES ,29X, WEIGHTED TIME-SERIES /)
      CALL PLOT (XR,XRW,1,500)
      DO291=1,LX
   29 G(I)=XRW(I)
      CALL FFT (XRW,XIW,-1.)
C     NOW WE ARE MULTIPLYING THE SIGNAL BY T
      DO9I=1,LX
      T=I-1
    9 XR(I)=T*G(I)*DT
C     NOW WE ARE COMPUTING THE PHASE
      CALL FFT (XR,XI,-1.)
      AVPH=0.
      LY=LX/2+1
      DO4I=1,LY
      VD=XRW(I)*XRW(I)+XIW(I)*XIW(I)
      XR(I)=-(XRW(I)*XR(I)+XIW(I)*XI(I))/VD
      AVPH=AVPH+XR(I)
```

```
    4   CONTINUE
        AVPH=AVPH/LY
        DO8I=1,LY
    8   XR(I)=XR(I)-AVPH
        PRINT350
  350   FORMAT(1X,AVPH)
        PRINT26,AVPH
   26   FORMAT(1X,5E16.8)
        AL=6.28318/(LX*DT)
        CALL QSF(AL,XR,XI,LY)
        L=LY-2
        DO7 I=1,L
        XI(LY+I)=-XI(LY-I)
    7   CONTINUE
        CALL POLAR (XRW,XIW)
        WRITE (6,31)
   31   FORMAT(1X,/22X, AMPLITUDE WEIGHTED TRANSFORM ,22X, PHASEUNWEIGHTED
       1TRANSFORM /)
        CALL MPLOT(XRW,XI)
        DO5I=1,LX
        AMPR(I)=ALOG(XRW(I))
        M(I)=AMPR(I)
    5   CONTINUE
        CALL FFT (AMPR,XI,1.)
        DO101I=1,LX
        S(I)=ABS(AMPR(I))
  101   S(I)=20.*ALOG10(S(I))
        PRINT650
  650   FORMAT(1X/24X, COMP CEPSTRUM ,45X, LOG COMP CEPSTRUM /)
        CALL MPLOT(AMPR,S)
C       NOW WE ARE PROCEEDING FOR WAVELET RECOVERY
        DO1051G=1,IN
        READ107,KA
  107   FORMAT(I3)
        WRITE(6,34)KA
   34   FORMAT(1X/1X, NUMBER OF POINTS USED ,I5/)
```

```
      KB=KA+1
      DO1I=1,KA
      AXR(I)=AMPR(I)
    1 AXI(I)=XI(I)
      DO2I=KB,LY
      AXR(I)=0.
    2 AXI(I)=0.
      LZ=LY+1
      DO9I=LZ,LX
      AXR(I)=AMPR(I)
    9 AXI(I)=XI(I)
      WRITE(6,32)
   32 FORMAT(1X/1X, RECOVERY OF SOURCE WAVE LET /)
      CALL WAVER(AXR,AXI)
      LYM=LY-50
      DO 11 I=KB,LYM
      BXR(I)=AMPR(I)
   11 BXI(I)=XI(I)
      LYM=LYM+1
      DO 20 I=LYM,LY
      BXR(I)=0.
      DO12I=1,KA
      BXR(I)=0.
   12 BXI(I)=0.
      DO13I=LZ,LX
      BXR(I)=0.
   13 BXI(I)=0.
      WRITE(6,33)
   33 FORMAT(1X/1X, RECOVERY OF TRANSMISSION FUNCTION /)
      CALL WAVER(BXR,BXI)
C     A STANDS FOR WEIGHTING CONSTANT
C     N STANDS FOR THE POWER RAISED TO TWO IN FFT PROGRAMME
C     MM STANDS FOR THE ACTUAL NUMBER OF THE SAMPLES
  105 CONTINUE
      STOP
      END
```

```
      SUBROUTINE MPLOT(XR,XI)
      DIMENSION XR(1024),XI(1024)
   10 FORMAT(1X,///)
      WRITE(6,10)
      CALL PLOT(XR,XI,1,512)
      RETURN
      END
```

```
      SUBROUTINE FFT(XR,XI,SIGN)
      DIMENSION XR(1024),XI(1024),M(15)
      COMMON A,N,MM,DOT,BLANK,LX
      DO 1 I=1,N
    1 M(I)=2**(N-I)
      DO 4L=1,N
      NBLOCK = 2**(L-1)
      LBLOCK = LX/NBLOCK
      LBHALF = LBLOCK/2
      K=0
      DO 4I BLOCK = 1, NBLOCK
      FK = K
      FLX = LX
      U=SIGN*6.2831853*FK/FLX
      WKR=COS(U)
      WKI=SIN(U)
      ISTART=LBLOCK*(BLOCK-1)
      DO2I=1,LBHALF
      J=ISTART+I
```

57

```
      JH=J+LBHALF
      QR=XR(JH)*WKR-XI(JH)*WKI
      QI=XR(JH)*WKI+XI(JH)*WKR
      XR(JH)=XR(J)-QR
      XI(JH)=XI(J)-QI
      XR(J)=XR(J)+QR
      XI(J)=XI(J)+QI
2     CONTINUE
      DO3I=2,N
      I I=I
      IF (K-M(I))4,3,3
3     K=K-M(I)
4     K=K+M(II)
      K=0.
      DO7J=1,LX
      IF(K-J)5,15,15
15    HOLDR=XR(J)
      HOLDI=XI(J)
      XR(J)=XR(K+1)
      XI(J)=XI(K+1)
      XR(K+1)=HOLDR
      XI(K+1)=HOLDI
5     DO6I=1,N
      II=I
      IF(K-M(I))7,6,6
6     K=K-M(I)
7     K=K+M(II)
      IF(SIGN)9,10,10
9     CONTINUE
      RETURN
10    DO8I=1,LX
      XI(I)=XI(I)/FLX
8     XR(I)=XR(I)/FLX
      RETURN
      END
```

```
      SUBROUTINE PLOT(XR,XI,LA,LB)
      DIMENSION XR(1024),XI(1024),R(21),P(21)
      COMMON A,N,MM,DOT,BLANK
      XRMAX=0.
      XRPNZ=0.0
      XIPNZ=0.0
      DO 11 I=LA,LB
      AX=ABS(XR(I))
      IF(AX-XRMAX)11,5,5
    5 XRMAX=AX
   11 CONTINUE
      XIMAX=0.
      DO 10 I=LA,LB
      AY=ABS(XI(I))
      IF(AY-XIMAX)10,35,35
   35 XIMAX=AY
   10 CONTINUE
      PRINT6,XRMAX,XIMAX
    6 FORMAT (7H XRMAX,E16.8,6H XIMAX,E16.8)
      PRINT8,XRPNZ,XIPNZ
    8 FORMAT(2F5.1///)
      PRINT200
  200 FORMAT(25X,21H.....40X,21H.....)
      DO15 I=LA,LB
      XR(I)=XR(I)/XRMAX
   15 XI(I)=XI(I)/XIMAX
C     WE ARE NOW GOING TO INSTRUCT THE COMPUTER TO READ THE BLANK SPACES
      DO3K=1,21
    3 R(K)=BLANK
      DO7M=1,21
    7 P(M)=BLANK
C     WE ARE NOW CHOOSING THE POINTS FOR PLOTTING
      DO 40 I=LA,LB
```

```
      IF(XRPNZ)21,22,23
21    K=20.*(XR(I)+1.0)+1.5
      GO TO 25
22    K=10.0*(XR(I)+1.0)+1.5
      GO TO 25
23    J=20.*(XR(I)+.05)+.5
25    IF(XIPNZ)26,27,28
26    M=20.*(XI(I)+1.)+1.5
      GO TO 30
27    M=10.*(XI(I)+1.)+1.5
      GO TO 30
28    M=20.*(XI(I)+.05)+.5
30    IF(M.GT.25.OR.K.GT.25)GO TO 50
      R(K)=DOT
      P(M)=DOT
      HOLDR=XR(I)
      XR(I)=XR(I)*XRMAX
      HOLDI=XI(I)
      XI(I)=XI(I)*XIMAX
      PRINT4,XR(I),(R(L),L=1,21),HOLDR,XI(I),(P(J),J=1,21),HOLDI
4     FORMAT(E16.8,2X,21A1,2X,E16.8,2X,E16.8,2X,21A1,2X,E16.8)
      R(K)=BLANK
40    P(M)=BLANK
50    PRINT51,K,M
51    FORMAT(214)
      RETURN
      END
```

```
      SUBROUTINE POLAR(XR,XI)
      DIMENSIONXR(1024),XI(1024)
      COMMON A,N,MM,DOT,BLANK,LX
      PI=3.14159265
      DO120I=1,LX
      AMP=SQRT(XR(I)*XR(I)+XI(I)*XI(I))
      PHZ=ATAN2(XI(I),XR(I))
      XR(I)=AMP
  120 XI(I)=PHZ
      RETURN
      END
```

```
      SUBROUTINE WAVER(XR,XI)
      DIMENSION XR(1024),XI(1024)
      COMMON A,N,MM,DOT,BLANK,LX,DT
      CALL FFT(XR,XI,-1.)
      WRITE(6,10)
```

```
 10  FORMAT(1X,/1X, WAVER***LOG FROM CEPSTRAL /)
     CALL MPLOT(XR,XI)
     KT=LX/2+1
     DO100I=1,KT
     XR(I)=EXP(XR(I))
100  CONTINUE
     DO 12 I=1,LX
     HOLDR=XR(I)*COS(XI(I))
     HOLDI=XR(I)*SIN(XI(I))
     XR(I)=HOLDR
     XI(I)=HOLDI
     LT=KT-2
     DO99I=1,LT
     XR(KT+I)=XR(KT-I)
     XI(KT+I)=-XI(KT-I)
 99  CONTINUE
     XI(KT)=0.
     XI(1)=0.
     WRITE(6,11)
 11  FORMAT(1X/1X, WAVER***FREQ LOG,REAL EVEN,IM/ ODD /)
     CALL MPLOT(XR,X)
     CALL FFT(XR,XI,1.)
     PRINT850
850  FORMAT(1X/18X,RECOVERED WEIGHTED TIME SIGNAL,40X,IMA PART/)
     XI(1)=1.
     CALL MPLOT(XR,XI)
     NOW WE ARE UNWEIGHTING THE WAVE LET
     P=1.
     DO 111 I=1,LX
     XR(I)=XR(I)*P
     P=P/A
111  CONTINUE
     PRINT 900
900  FORMAT(1X/18X,RECOVERED UNWEIGHTED WAVELET,44X,IMA PART/)
     CALL MPLOT(XR,XI)
     RETURN
     END
```

APPENDIX II

MARINE SEISMIC REAL DATA

```
C     MARINE SEISMIC REAL DATA
-.22175E 01-.22939E 01-.86355E 00 .20674E 01 .44365E 01 .35117E 01 .56079E 00
-.12629E 01-.13945E 01-.81323E 00 .64331E 00 .90381E 00-.12979E 01-.28369E 01
-.71265E 00 .14053E 01 .88394E 00-.11719E 00 .77661E 00 .14570E 01 .20972E 00
-.15227E 01-.10889E 01 .99438E 00 .23752E 01 .23320E 01 .29004E 01 .34473E 01
 .23826E 01 .14526E 00-.14031E 01-.91333E 00 .90308E 00 .27100E 01 .33750E 01
 .22734E 01-.26343E 00-.26523E 01-.24570E 01 .20630E 00 .24238E 01 .18760E 01
-.47754E 00-.20664E 01-.14141E 01 .10627E 01 .29717E 01 .16799E 01-.31113E 01
-.13645E 02-.34688E 02-.57625E 02-.60063E 02-.26098E 02 .19758E 02 .16227E 02
-.83703E 02-.23019E 03-.22175E 03 .95750E 02 .43113E 03 .26650E 03-.19294E 03
-.35906E 02 .02775E 03 .12923E 04 .98721E 03 .82215E 03 .70631E 03-.61025E 03
-.25530E 04-.26580E 04-.12953E 04-.45609E 02-.31250E 03-.99975E 03-.68000E 03
 .57513E 03 .15798E 04 .15455E 04 .68025E 03-.17763E 03-.23069E 03 .51238E 03
 .12060E 04 .11165E 04 .44256E 03 .63266E 02 .40031E 03 .76813E 03 .24963E 03
-.10175E 04-.19420E 04-.17490E 04-.80875E 03-.72188E 02 .17727E 03 .47538E 03
 .96225E 03 .92000E 03-.19473E 02-.99500E 03-.91375E 03 .95875E 02 .89475E 03
 .73794E 03-.87328E 02-.74750E 03-.55075E 03 .40438E 03 .10308E 04 .38869E 03
-.99050E 03-.16625E 04-.10053E 04 .25638E 03 .10328E 04 .90200E 03 .33019E 03
 .37051E 02 .10505E 03 .47363E 02-.23719E 03-.24356E 03 .26494E 03 .81075E 03
 .86850E 03 .44188E 03-.15369E 03-.57825E 03-.57600E 03-.20563E 03 .10100E 03
-.34438E 02-.52775E 03-.93825E 03-.82550E 03-.11898E 03 .62688E 03 .70875E 03
 .21613E 03-.31316E 02 .29631E 03 .55400E 03 .19739E 03-.31031E 03-.26063E 03
 .13800E 03 .14444E 03-.29650E 03-.49950E 03-.13300E 03 .32556E 03 .35981E 03
 .48000E 02-.26506E 03-.44825E 03-.47606E 03-.20919E 03 .34806E 03 .80450E 03
 .78794E 03 .40219E 03-.52219E 02-.50700E 03-.85525E 03-.66950E 03 .23394E 03
 .11515E 04 .10465E 04-.16675E 03-.13113E 04-.12315E 00-.14431E 03 .74300E 03
 .68225E 03 .12445E 04-.51950E 03-.53125E 03-.77813E 02 .56444E 03 .99225E 03
 .82425E 03 .26730E 02-.92050E 03-.12875E 04-.67125E 03 .54738E 03 .13350E 04
 .96500E 03-.13000E 03-.89729E 03-.92850E 03-.52750E 03 .15169E 03 .99025E 03
 .12788E 04 .47219E 03-.66300E 03-.94675E 03-.48569E 03-.19513E 03-.89938E 02
 .43938E 03 .99400E 03 .39500E 03-.12073E 04-.19580E 04-.72100E 03 .12645E 04
 .19383E 04 .79525E 03-.92025E 03-.17411E 04-.10293E 04 .66000E 03 .19893E 04
 .19638E 04 .74094E 03-.62075E 03-.14531E 04-.14895E 04-.70550E 03 .44000E 03
 .10430E 04 .72431E 03 .24436E 02-.53650E 03-.96700E 03-.10588E 04-.28394E 03
 .99800E 03 .14478E 04 .50938E 03-.60725E 03-.75975E 03-.94013E 02 .51944E 03
 .70100E 03 .46419E 03-.19063E 03-.99775E 03-.13078E 04-.74925E 03 .31181E 03
 .11943E 04 .14365E 04 .80525E 03-.54756E 03-.17038E 04-.15210E 04-.32594E 02
```

```
 .13593E 04 .15385E 04 .76319E 03-.16169E 03-.81850E 03-.92700E 03-.26581E 03
 .64444E 03 .78563E 03 .10505E 02-.71325E 03-.71525E 03-.34369E 03-.21270E 02
 .35806E 03 .71588E 03 .51531E 03-.30831E 03-.96800E 03-.81700E 03-.57266E 02
 .75419E 03 .11985E 04 .93925E 03-.46680E 01-.90700E 03-.98175E 03-.36456E 03
 .20500E 03 .42606E 03 .44275E 03 .19917E 03-.35106E 03-.70325E 03-.31950E 03
 .46238E 03 .78950E 03 .45313E 03-.22871E 02-.34338E 03-.63975E 03-.72900E 03
-.16100E 03 .80275E 03 .11920E 04 .56925E 03-.43750E 03-.10053E 04-.88850E 03
-.29331E 03 .40475E 03 .73906E 03 .47763E 03-.51609E 02-.34794E 03-.33944E 03
-.22669E 03-.21160E 02 .26744E 03 .33119E 03 .16008E 02-.26713E 03-.14256E 03
 .11872E 03 .17142E 03 .24338E 03 .50925E 03 .43675E 03-.36475E 03-.11675E 04
-.96600E 03 .98531E 02 .94225E 03 .93050E 03 .35613E 03-.26744E 03-.69550E 03
-.76350E 03-.35694E 03 .28725E 03 .68169E 03 .59331E 03 .18227E 03-.28150E 03
-.53350E 03-.35625E 03 .12447E 03 .41806E 03 .25413E 03-.78125E 02-.22825E 03
-.23544E 03-.19981E 03 .31699E 02 .44713E 03 .57294E 03 .98969E 02-.51925E 03
-.60450E 03-.16644E 01 .26088E 03 .42881E 03 .43019E 03 .21794E 03-.25556E 03
-.62950E 03-.49456E 03-.12402E 02 .33400E 03 .36819E 03 .20294E 03-.84484E 02
-.37413E 03-.38775E 03-.25574E 02 .39125E 03 .49318E 03 .27281E 03-.70313E 02
-.39350E 03-.52700E 03-.25682E 03 .30631E 03 .63244E 03 .38544E 03-.10616E 03
-.33388E 03-.28369E 03-.22788E 03-.15169E 03 .11759E 03 .41556E 03 .37506E 03
-.96406E 01-.34756E 03-.36325E 03-.14356E 03 .10466E 03 .25631E 03 .23363E 03
 .35758E 02-.17406E 03-.21300E 03-.90141E 02 .74125E 02 .21731E 03 .25719E 03
 .55219E 02-.30094E 03-.41650E 03-.10428E 03 .27950E 03 .34231E 03 .19028E 03
 .88719E 02-.48625E 02-.36656E 03-.56725E 03-.25881E 03 .34050E 03 .60644E 03
 .35094E 03-.29023E 02-.21075E 03-.24461E 03-.20975E 03-.65891E 02 .99094E 02
 .89875E 02-.67913E 02 .0    E    .0    E    .15108E 03 .24494E 03 .23675E 03
 .88406E 02-.17081E 03-.34588E 03-.28450E 03-.87719E 02 .82203E 02 .23763E 03
 .37338E 03 .27363E 03-.14269E 03-.50406E 03-.41394E 03-.35928E 02 .19223E 03
 .19844E 03 .21075E 03 .22775E 03 .70461E 02-.16369E 03-.18525E 03 .11895E 02
 .15620E 03 .11900E 03-.27793E 01-.13581E 03-.24598E 03-.20200E 03 .50844E 02
 .27238E 03 .18856E 03-.10767E 03-.29906E 03-.27063E 03-.11166E 03 .13703E 03
 .41606E 03 .49200E 03 .22119E 03-.15961E 03-.31781E 03-.25338E 03-.16081E 03
-.54297E 02 .13264E 03 .24215E 03 .59705E 02-.27188E 03-.35788E 03-.83016E 02
 .24750E 03 .33198E 03 .17813E 03-.31383E 02-.15375E 03-.11438E 03 .51859E 02
 .17786E 03 .14409E 03 .40574E 02-.12672E 02-.66172E 02-.18744E 03-.24750E 03
-.10586E 03 .11517E 03 .18614E 03 .91797E 02-.25816E 02-.12825E 03 .0
-.13638E 03 .16141E 03 .0    E    .0    E   -.13763E 03-.34306E 03-.20381E 03
 .41894E 02 .16523E 03 .15700E 03 .70109E 02-.62688E 02-.15388E 03-.11947E 03
```

```
-.11914E 02 .56828E 02 .71859E 02 .65641E 02 .10687E 02-.91031E 02-.11798E 03
 .72988E 01 .15647E 03 .16961E 03 .91375E 02 .47742E 02 .27881E 01-.12306E 03
-.20594E 03-.80641E 02 .12955E 03 .15775E 03 .39297E 01-.98547E 02-.75016E 02
-.62406E 02-.10239E 03-.72063E 02 .56016E 02 .15286E 03 .67781E 02-.42016E 02
-.76016E 02-.31980E 02 .39477E 02 .10192E 03 .10398E 03 .17590E 02-.31563E 02
-.93172E 02-.32453E 01 .27465E 02 .85281E 02 .14197E 03 .10248E 03-.70969E 02
-.21156E 03-.15238E 03 .15594E 02 .86156E 02 .47770E 02 .41281E 02 .78844E 02
 .38035E 02-.77984E 02-.11020E 03-.99102E 01 .77188E 01 .52266E 02-.52217E 01
-.11414E 02-.78203E 01-.35391E 02-.43625E 02-.34217E 01 .26047E 02 .89656E 01
-.19176E 02-.37453E 02-.53625E 02-.33109E 02 .55958E 02 .13845E 03 .10814E 03
 .18784E 01-.50359E 02-.39047E 02-.61938E 02-.10250E 03-.44281E 02 .84234E 02
 .11169E 03 .94736E 01-.58688E 02-.17672E 02 .15637E 02-.25352E 02-.38297E 02
 .37172E 02 .96156E 02 .56344E 02-.80830E 01-.15867E 02-.18035E 01-.13711E 02
-.26820E 02-.31004E 02-.61438E 02-.90859E 02-.39563E 02 .69078E 02 .11897E 03
 .89125E 02 .61266E 02 .38836E 02-.48125E 02-.14450E 03-.10383E 03 .47324E 02
 .11306E 03 .36055E 02-.31340E 02-.85264E 01 .10962E 00-.63078E 02-.92672E 02
-.24336E 02 .47973E 02 .44434E 02 .15930E 02 .17359E 02 .22617E 02 .19914E 02
 .38820E 02 .52761E 02 .29020E 02-.81563E 02-.91078E 02-.24875E 02 .32887E 02
 .69172E 02 .11911E 03 .12720E 03 .17986E 02-.12625E 03-.15163E 03-.73438E 02
-.31301E 02-.37813E 02 .12223E 02 .10547E 03 .10591E 03-.44360E 00-.66484E 02
-.23824E 02 .28691E 02 .14613E 02-.14861E 02-.76348E 01 .76895E 01 .10661E 02
 .27686E 02 .52375E 02 .38969E 02-.11902E 02-.57188E 02-.89813E 02-.11888E 03
-.10106E 03-.22871E 01 .99266E 02 .10089E 03 .31379E 02-.53828E 01-.21738E 01
-.19879E 02-.34391E 02 .20066E 02 .92621E 02 .71438E 02-.18652E 02-.43391E 02
 .16484E 02 .39098E 02-.26152E 02-.65844E 02-.68438E 02-.20789E 02-.53145E 01
-.10691E 02-.50664E 01 .92314E 01 .25297E 02 .41051E 02 .34352E 02-.90234E 01
-.47484E 02-.32469E 02 .12238E 02 .30984E 02 .29441E 02 .44270E 02 .48668E 02
-.47939E 01-.72344E 02-.68891E 02-.10707E 02 .10390E 02-.16754E 02-.17675E 02
 .20160E 02 .27000E 02-.12711E 02-.27836E 02 .12695E 02 .48703E 02 .32355E 02
-.59805E 01-.20880E 02-.14145E 02-.30361E 01 .11617E 02 .21805E 02 .93467E 01
-.19176E 02-.39609E 02-.47359E 02-.47001E 02-.21977E 02 .30555E 02 .60703E 02
 .30285E 02-.17191E 02-.19883E 02 .50066E 01 .23574E 01-.14430E 02 .10269E 02
 .56828E 02 .45648E 02-.28055E 02-.73219E 02-.40500E 02 .12501E 02 .22117E 02
-.29468E 00-.15879E 02-.20777E 02-.23281E 02-.14717E 02 .85068E 01 .31809E 02
 .43645E 02 .42074E 02 .22633E 02-.88965E 01-.25023E 02-.10828E 02 .83730E 01
 .66582E 01-.79858E 00 .52285E 01 .11345E 01-.34984E 02-.63219E 02-.31227E 02
 .28039E 02 .32348E 02-.20430E 02-.46703E 02-.97305E 01 .35188E 02 .42969E 02
```

```
 .38621E 02 .48098E 02 .48730E 02 .19426E 02-.20613E 02 .0          .0
-.18742E 02 .68486E 01 .0          .0          -.47609E 02-.42500E 02-.19758E 02
 .15088E 01 .28926E 02 .60141E 02 .61109E 02 .19352E 02-.18465E 02-.10566E 02
 .17590E 02 .18234E 02-.25879E 00-.43359E 00 .88057E 01-.10727E 02-.49453E 02
-.55766E 02-.17848E 02 .19301E 02 .19902E 02-.41953E 01-.24953E 02-.23578E 02
 .40918E 01 .39285E 02 .51734E 02 .36901E 02 .20063E 02 .14238E 02 .17358E 00
-.19422E 02-.12469E 02 .23770E 02 .39945E 02 .93330E 01-.30543E 02-.43047E 02
-.43078E 02-.40625E 02-.37297E 02 .61191E 01 .40207E 02 .21359E 02-.25250E 02
-.39281E 02-.73613E 01 .32504E 02 .48691E 02 .39750E 02 .16715E 02-.77236E 01
-.20512E 02-.17387E 02-.35283E 01 .16316E 02 .33652E 02 .26328E 02-.16051E 02
-.60 16E 02-.62141E 02-.24668E 02 .48311E 01 .68525E 01 .88008E 01 .23742E 02
 .24992E 02 .34803E 01-.72656E 01 .13100E 02 .36176E 02 .28742E 02 .63696E 00
-.19391E 02-.26809E 02-.30453E 02-.23891E 02-.75195E-01 .23922E 02 .23086E 02
-.59521E 01-.42953E 02-.57672E 02-.29262E 02 .25207E 02 .56859E 02 .39949E 02
 .46631E 01-.10109E 02-.78164E 01-.86455E 01-.40117E 01 .21543E 02 .44332E 02
 .24336E 02-.27852E 02-.56203E 02-.33781E 02 .57803E 01 .23469E 02 .17785E 02
 .40576E 01-.12746E 02-.28848E 02-.31172E 02-.11656E 02 .10785E 02 .38816E 02
 .34656E 02 .90635E 01-.19004E 02-.27570E 02-.11109E 02 .11453E 02 .20102E 02
 .18113E 02 .12145E 02-.68135E 01-.35313E 02-.41516E 02-.75645E 01 .32453E 02
 .33492E 02-.26538E 00-.26930E 02-.27273E 02-.14504E 02-.15920E 01 .17582E 02
 .32727E 02 .24293E 01-.66787E 01-.34656E 02-.36656E 02-.13973E 02 .15293E 02
 .31066E 02 .25129E 01 .73810E 01-.47393E 01-.40604E 01-.15754E 01-.29785E-01
 .66572E 01 .17445E 02 .12324E 02-.16773E 02-.41094E 02-.31020E 02-.11770E 01
 .13672E 02 .84971E 01 .17520E 01-.33096E 01-.14813E 02-.21926E 02-.24795E 01
 .36527E 02 .57250E 02 .37230E 02-.37920E 01-.31176E 02-.32203E 02-.15934E 02
 .39951E 01 .17867E 02 .19508E 02 .81465E 01-.10973E 02-.28805E 02-.34188E 02
-.19379E 02 .77227E 01 .22230E 02 .96191E 01-.12828E 02-.16777E 02-.61011E 00
 .14750E 02 .19480E 02 .20234E 02 .16055E 02-.14614E 01-.24777E 02-.27078E 02
-.67920E 00 .26656E 02 .26777E 02 .49414E 01-.15570E 02-.26715E 02-.31164E 02
-.22652E 02 .21387E 01 .28609E 02 .36901E 02 .23160E 02 .10828E 01-.12914E 02
-.87852E 01 .85859E 01 .20410E 02 .12805E 02-.64023E 01-.18367E 02-.20188E 02
-.22227E 02-.23230E 02-.10250E 02 .11567E 02 .17609E 02 .19082E 01-.88408E 01
 .28701E 01 .19715E 02 .21621E 02 .15594E 02 .15094E 02 .12234E 02-.35625E 01
-.10281E 02-.12113E 02 .61738E 01 .19484E 02 .13039E 02-.39424E 01-.21996E 02
-.30934E 02-.22711E 02-.38066E 01 .88391E 01 .10922E 02 .10398E 02 .78760E 01
-.36404E 01-.15688E 02-.98672E 01 .90332E 01 .15809E 02 .55654E 01 .55859E 00
 .10196E 02 .16797E 02
```

76

BIBLIOGRAPHY

1. Ananthapadmanabha, T.V. and Yegnanarayana, B., 1975 Epoch Extraction of Voiced Speech, IEEE Trans. on ASSP, Vol.23, No.6, Dec.1975, pp.562-570.

2. ---------- 1976 A decomposition Technique for Composite Signal, IEEE, Vol.24, no.6 pp.612-620.

3. ---------- 1976 Epoch Extraction of Composite Signals, IEEE, 1976, Vol-22, No.11, pp.718-720.

4. Deekun, H.M., 1969 Ocean Reverberations - Their nature and elimination, Geophy., Vol.34, No.2, pp.233-261.

5. Bergland, G.D., 1969 A guided tour of the fast Fourier transform, IEEE Trans. on Spectrum, Vol.6, No.7 pp.41-52.

6. Bogert, B.P., Healy, M.J. and Tukey, J.W., 1963 The quefrency analysis of time series for echoes, cepstrum, Proc. Symp. on Time Series Analysis, Edited by M.Rosenblatt., New York, Wiley, pp.209-243.

7. Bogert, B.P., 1963 The Normalized Cepstrum analysis of a stationary complex echoed gaussian signal in stationary gaussian noise, IEEE Trans. IT., Vol.6, No. 6, pp.338-343.

8. Dahl, P., Steffe, P.L. and Bergan, G.M., 1974 The application of homomorphic filtering to shallow water seismology, Part I - Methods, Geophy.Vol.39, no. - 4 pp.481-510.

9. ---------- 1974 ----------, Part II Real Data, 17-33.

[illegible] the [illegible] Geophy. Vol.39,

11. Dutchen, B., 1976 Homomorphic Filtering - Theory and Practice, GP., Vol.23, No.4, pp.712-742.

12. Childers, D.G., Varga, R.S. and Perry, Jr. N.C., 1970 Composite Signal Decomposition, IEEE Trans.AES, 1970, AU-18, No.4, pp.471-477.

13. Childers, D.G. and Kemerait, R.C., 1972 Signal detection and extraction by Cepstrum techniques, IEEE Trans. IT., 1972, Vol.IT-18, No.6 pp.746-753.

14. Claerbout, J.F. and Robinson, E.A., 1964 The error in least squares inverse filtering, Geophy., Vol.29, No.1, pp.43-120.

15. Dobrin, M.B., 1960 Introduction to Geophysical Prospecting, McGraw Hill Book Co., INC., New York, pp.1- 163.

16. Ellsworth, T.P., 1963 Multiple Reflections, Geophy. Vol.15, No.1, 1963, pp.1-30.

17. Gold, B. and Rader, C.M., 1969 Digital Processing of Signals, McGraw Hill Book Co., New York.

18. Goodyear, C.E., 1971 Signal and Interpretation, Butterworths, London.

19. Goupillaud, P.L., 1961 An approach to inverse filtering of near surface layer effects from seismic records, Geophy. Vol.26, No.4 pp.754-760.

20. Gupta, M.M., 1965 Reflection of plane waves from a linear transition layer in liquid media, Geophy., Vol.30, No.1, pp.122-128.

21. Gurvich, I., 1970 Seismic Prospecting, Mir Publishers, Moscow.

23. Jury, E.I., 1964. Theory and Application of z - transform method, John Wiley and Sons, INC., New York.

24. Kanasevich, E.R., 1973 Time sequence analysis in Geophysics, The University of Alberta Press, Canada.

25. Kopec, G.E., Oppenheim, A.V. and Tribbot, J.M., 1977 Speech analysis by Homomorphic Prediction, IEEE Trans. on ASSP, Vol.25, No.1, Feb. 1977, pp.40-43.

26. Lathi, B.P., 1965 Communication Systems, John Wiley and Sons, INC., New York.

27. Lee, Y.W., 1960 Statistical Theory of Communication, John Wiley and Sons, INC, New York.

28. Limaeth, R.O., 1969 A review on recent adv mood in digital processing of Geophysical data.

29. Linse, L.N., 1971 A note on the application of Wiener multichannel deconvolution, Jour. of the Canadian Soc. of E.G.Sts., 1974, Vol.10, No.1, Dec.1973, pp.65-71.

30. Liu, C.L. and Liu, J.W.S., 1975 Linear Systems Analysis, McGraw Hill Book Co., INC, New York.

31. Oppenheim, A.V., 1966 (a) Superposition in a class of nonlinear systems, Res. Lab. of Electronics, MIT, Tech., Report, 432.

32. ---------- 1966 (b) Homomorphic Filters, Res. Lab. of Electronics, MIT, Quart. Prog. Rep. 77, pp.258-260.

33. Oppenheim, A.V., Schafer, R.W. and Stockham, T.J., 1968 Nonlinear Filtering of multiplied and convolved signals, Proc., IEEE, Vol.56, No.8, pp.1264-1291.

37. Papoulis, A., 1962 The Fourier integral and its applications, McGraw Hill Book Co., Inc., New York.

38. Peacock, K.L. and Treitel, S., 1969 Predictive Deconvolution Theory and Practice, Geophy. Vol.34, No.2 pp.155-169.

39. Pipes, L.A., 1940 Applied Mathematics for Engineers and Physicists, McGraw Hill Book Co., Inc., New York.

40. Rayhel, R., 1975 Correspondence on Spectrum of two dimensional functions, IEEE Trans., Vol.21, No.5 pp.516-517.

41. Ray, C.H., 1977 Wavelet Estimation - The science of wavelet processing, Paper presented at the 47th Annual meeting of the SEG in Houston, Texas.

42. Rice, R.B., 1962 Inverse Convolution Filters, Geophy. Vol.27, No.1, pp.4-18.

43. Riker, N., 1953 The form and laws of propagation of Seismic wavelets, Geophy. ~~1953~~, Vol.18, No.1 pp.10-30.

44. ---------- 1953 Wavelet contraction, Wavelet expansion and the control of seismic resolution, Geophy., ~~1953~~, Vol.18, No.6 pp.769.

45. Robinson, E.A., 1957 Predictive Decomposition of Seismic Traces, Geophy. Vol.22, No.4, pp. 392-413

46. Robinson, E.A., 1963 Multichannel z - transform and Minimum delay, Geophy. Vol.31, No.3, 482-500.

47. Robinson, E.A. and Treitel, S., 1964 Principle of digital filtering, Geophy. Vol.29, No.3, pp.395-404.

44. Robinson, E.A. and Treitel, S., 1967 Principles of digital Wiener Filtering, GP., Vol.15, No.3, pp.311-333.

45. Savarensky, E., 1975 Seismic Waves, Mir Publishers, Moscow.

46. Schafer, R.W., 1969 Echo removal by Discrete Generalized Linear Filtering, Res. Lab. of Electronics, MIT Tech. Report 468.

47. Schneider, W.A., Larner, K.L., Burg, J.P., and Backus, M.M., 1964 A new data processing technique for the elimination of ghost arrivals on reflection seismograms, Geophy., Vol.29, No.5, pp.783-803.

48. Shanks, R.K., 1970 Theory and Applications of Homomorphic Filtering to Seismograms, (Unpublished) M.Tech. Diss. UBC, 1970.

49. Silverman, D., 1967 The digital processing of seismic data, Geophy., Vol.32, No.6, pp.1003-1008.

50. Tribolet, J.M., 1977 A new phase unwrapping algorithm, IEEE Trans. on ASSP., Vol.25, No.2, April 1977, pp.170-177.

51. Treitel, S., 1963 Theoretical seismogram with frequency and depth dependent absorption, Geophy., Vol.28, No.6, pp.703-705.

52. Treitel, S. and Robinson, E.A., 1964 Seismic wave propagation in layered media in terms of communication theory, Geophy., Vol.29, No.1, pp.17-23.

53. Treitel, S. and Robinson, E.A., 1977 Deconvolution - Homomorphic or Predictive ? IEEE Trans. on Geoscience Electronics, Jan 1977, Vol. 16, No pp.11-19.

64.	Ulrych, T.J. and Lacoste.	1969	Minimum Phase, Jour. Can. Soc. Expl. Geophysicists, V.5, pp.28-32. (Vol. 2, No. 1)
65.	Ulrych, T.J.,	1971	Application of Homomorphic Deconvolution to Seismology, Geophy., Vol.36, No.6, pp.650-660.
66.	Ulrych, T.J., Jones, O.C. and Canavillo, P.C.,	1973	Homomorphic Deconvolution of Some Teleseismic Events, BSSA, Vol.63, No.5, pp.1969-1981.
67.	Worth, G.S., Liu, D.T. and Stoffa, A.M.,	1969	Offshore Siting - Field experiments and theoretical interpretation, Geophy. Vol.34, No.5, pp.650 - 662.
68.	Whalen, D.A.,	1971	Detection of Signals in Noise, Academic Press, New York and London.

- . -